Westfälische Wilhelms-Universität Münster

Institute of Theoretical Physics

Bachelor's thesis

Gluino stop co-annihilations in the Minimal Supersymmetric Standard Model

Bastian Ottensmann

b_otte03@uni-muenster.de

AG Klasen

Supervisor and first examiner: Priv. Doz. Dr. K. Kovařík

Second examiner: Prof. Dr. M. Klasen

August 18, 2020

Declaration of Academic Integrity

I hereby confirm that this thesis on Gluino stop co-annihilations in the Minimal Supersymmetric Standard Model is solely my own work and that I have used no sources or aids other than the ones stated. All passages in my thesis for which other sources, including electronic media, have been used, be it direct quotes or content references, have been acknowledged as such and the sources cited.

_____
(date and signature of student)

I agree to have my thesis checked in order to rule out potential similarities with other works and to have my thesis stored in a database for this purpose.

_____
(date and signature of student)

Contents

1. Introduction

Many experiments in the past century gave strong evidence for the existence of non-baryonic cold dark matter with a critical density $\Omega_c h^2 = 0.120 \pm 0.001$. Since the Standard Model (SM) of particle physics does not provide a suitable candidate for dark matter, this model needs to be extended.
One idea is to postulate a supersymmetry (SUSY) which relates all bosons and fermions by a supersymmetric operation. This results in the existence of superpartners for all particles of the Standard Model where those superpartners have the same quantum numbers as the SM particles and a spin differing by $1/2$. A low-energy supersymmetry provides a solution for the hierarchy problem which is an important benefit of supersymmetric theories.
The Minimal Supersymmetric Standard Model (MSSM) extends the Standard Model with characteristics of supersymmetry in a minimal way. By demanding the conservation of R-parity, the MSSM includes the lightest neutralino as a suitable candidate for dark matter as a Weakly Interacting Massive Particle (WIMP). The WIMPs are in equilibrium in the early universe and their annihilations "freeze out" when the Hubble expansion rate is getting larger than the annihilation rate. At this time, the annihilation processes are not efficient enough anymore to sustain the WIMPs in equilibrium, they thus fall out of equilibrium. After a short time, comoving number density of the WIMPs remains constant which results in the relic density. The time evolution of the number density is described quantitatively by the Boltzmann equation so the numerical solution of this equation provides the relic density.
In this thesis the co-annihilation of the supersymmetric particles gluino and scalar top quark into a gluon and a top quark is analysed. The goal is to obtain the cross section for this process at tree-level by an analytic calculation of the squared invariant amplitude and obtain the total cross section of the process by implementing the analytic result into the code **DM@NLO**. Since many parameters of the MSSM are not constrained by the theory, one has to choose them compatible with experimentally detected relic density. A scenario with parameters chosen in such a way that the analysed process gives the most contribution to the relic density is studied by calculating the corresponding total cross section. Furthermore, the contributions of the different channels to the total cross section are determined.

2. Evidence for existence of Dark Matter

In the 1930s, first publications suggested that there is some kind of invisible matter in galaxies and clusters but most of astronomical data agreed with the classical cosmological picture until the 1970s. Then, experimental data on the redshift of light emitted from all bright galaxies became available. Analyses of this data did not agree with the classical expectation but introducing the existence of dark matter as dominating part of the universe helped to solve this and many other problems at once.
The measurement of cosmic microwave background fluctuations by COBE satellite, which were at least two order of magnitudes lower than expected, finally led to the assumption that global dark matter must be non-baryonic [Ein09, p. 1-2]. This chapter is based on "Dark Matter" by J. Einasto [Ein09].

2.1. Rotation curves and stability of galaxies

By observing galaxies and their rotation curves one can infer its mass distribution. To be more specific, when most of a galaxy's mass is localized in its center, the velocity decreases with radial distance r from center by Kepler's laws. In our solar-system the mass is mostly present in the sun, therefore one observes the velocity of planets to decrease with rising r.
As an example, we look at the rotation curve of M31, the Andromeda galaxy. In fig. 1 we show the interpolated rotation curve of M31 by Roberts and Whitehurst(1975) where the cumulative mass was determined by the rotation velocity data. This data suggests that rotation velocities in this galaxy are mostly constant for radial distances r of 16-30 kpc. The mass distribution in the galaxy thus might rise linear with r. Due to use of photometric data it was possible to determine the distribution of light and by making use of both light distribution and the total mass distribution, the Mass-to-luminosity ratio M/L was calculated. Consequently, in the peripheral region from 20-30 kpc of M31 M/L was established to roughly 200 [Ein09, p. 4]. Therefore, a high total mass with a low luminosity is needed in this region.
Calculating the mass distribution by the rotation velocity led to similar results with increasing M/L in the periphery of other galaxies, too. Since these peripheries mostly contain old metal-poor halo-type stellar populations with low $M/L \approx 1$, there might be another population with very high M/L or rotation velocities might be disturbed by non-circular motions [Ein09, p. 4].

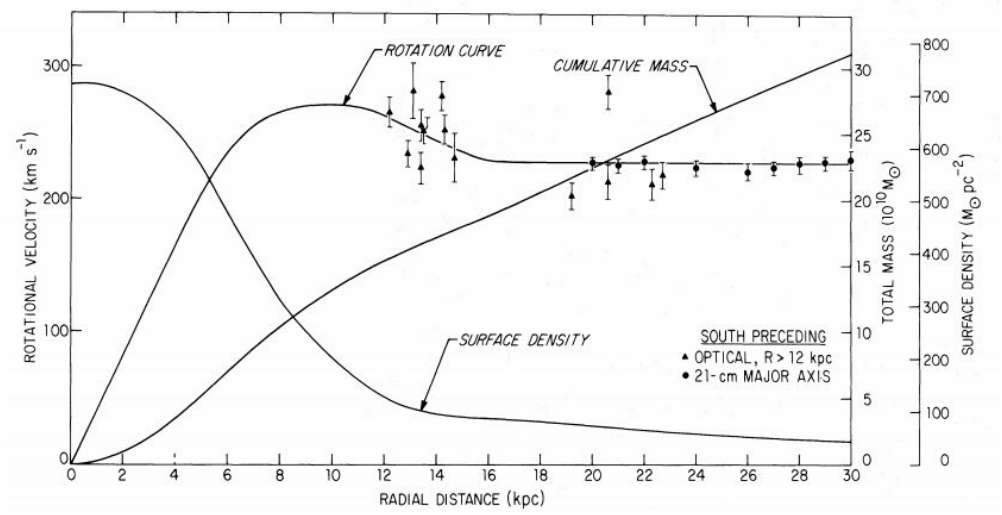

Figure 1: Rotation curve, cumulative mass and surface density by Roberts and Whitehurst(1975) of M31 for radial distances up to 30 kpc. [RW75]

A numerical analysis of the stability of galaxies was done by Peebles and Ostriker in 1973 [OP73]. They used different models in order to study the stability of highly flattened disks which are primarily supported by rotation. In their calculations, they discovered that cold, axisymmetric and flat galaxies are unstable and tend to develop barlike structures. Referring to Kalnajs'(1973), who constructed stable models until a critical value of $t \approx 0.14$ ('kinetical rotation energy'/'gravitational energy'), Peebles and Ostriker conclude that there are three ways to construct such systems. First, they suggested a hot flat disk that heats up until t is approximately 0.14 which does not agree with observations of flat spiral galaxies. Second, a cold rotating bar could evolve where random motions are less significant than streaming ones but that seems not to be a suitable model for a not barred spiral galaxy.
Finally, their favored theory for our galaxy was adding another hot disk component which must have a large mass, large radial orbits and remains unseen. Masses of this new component - called halo - are required to be equal or greater than the disk's mass to stabilize the flat galaxy.

2.2. Gravitational lensing

Since dark matter does not interact electromagnetically but by gravitation, the geometry of space-time can help to find dark matter. Dark matter bends spacetime by gravitation and for this reason light follows this curvature of spacetime. The effect of gravitational lensing appears when gravitating mass bends light propagating between an observer and a distant object.
Dense mass concentrations like centers of galaxies or clusters of galaxies cause strong gravitational lensing and are easy to observe. The bending of space-time is there so strong that light can take multiple ways around the lens. Consequently, the observer sees the distant object multiple times under slightly different angles. Positions and shapes of these images are utilized to determine the distribution of mass causing this effect.
If the distant object is directly behind a circular lens, the light can travel alongside any edge of it. As a result, the object appears as an "Einstein Ring". The size of this ring is proportional to the mass causing this lensing effect [MKR10, p. 4]. Less strong forms like weak lensing, where small distortions of many background objects need to be detected, are used for determination of mass distributions of clusters and superclusters. Fischer and Tyson, for instance, analysed the X-ray cluster RXJ 1347.5-1145 [FT97, p. 1]. They concluded a lensing mass almost twice as high as results previously obtained by analysing X-ray data.

Besides this, MAssive Compact Halo Objects (MACHOs) as well as white and brown dwarfs are mostly invisible but can be detected by microlensing effects. When a MACHO passes in front of a star, the star shines brighter because the light is deflected by gravity. According to Einasto, some authors predicted a maximum of 20% of dark matter in our galaxy might consists of brown or white dwarfs. Hubble Space telescope's NICMOS instrument, though, revealed that 6% of stellar mass is in brown dwarfs. In regards to the whole matter of our universe, this portion might be neglected[Ein09, p. 10].

2.3. Fluctuations in CMB

The observation of CMB provides information on the universe at the time of recombination where baryonic gas became neutral. By gravitational clustering in the early universe after recombination, density fluctuations were able to grow by gravitation. Models showed that the formation of structures like galaxies, clusters and superclusters needed density fluctuations in the order of 10^{-3} in the density [Ein09, p. 12]. It was also established that temperature fluctuations were required to be of the same order. For this reason the observation of temperature fluctuations in cosmic microwave background, which is a relic of the time before recombination, makes it possible to compute the density fluctuations of baryonic matter at that time.
In the 1970s, the observation of CMB showed that limits for temperature fluctuations are much lower than expected. As a result, non-baryonic dark matter is required for structure formation. In a dark matter dominated medium perturbations might start earlier than in a baryonic dominated one so that density fluctuations at the time of recombination are sufficient for formation of structures.

2.4. Dark Matter candidates

Initially, in the 1970s, the "pancake" theory by Zeldovich and the hierarchical clustering theory by Peebles tried to explain mechanisms of structure formation. Zeldovich suggested that matter first gathered in "pancakes" and then broke up into smaller structures. In contrast, hierarchical clustering assumed that smaller scale structures form first. After that, clustering would cause larger scale structures[Ein09, p. 15].
The availability of first all-sky complete redshift surveys of galaxies[ddC76] made it possible to determine the three-dimensional distribution of galaxies. It showed that galaxies and clusters are arranged in one-dimensional systems with space between those nearly empty. Numerical studies by the group around Zeldovich established similar results: high-density cells are enclosed by large under-dense regions so dense regions might be assumed as "pancakes".
According to Einasto [Ein09, p. 16-17] though, significant differences remained between the "pancake" model and observations. To be more specific, the original "pancake" model predicts superclusters with a diffuse forms, but in fact superclusters are made of several interweaved filaments. This is because the original model used the idea of neutrino-dominated dark matter where small-scale fluctuations are rinsed out by neutrinos' high velocity.
Additionally, neutrino-dominated theories predict galaxy and supercluster formation to take place at a later time than old stellar populations suggest. Cold dark matter theories where the dark matter particles move slowly and small-scale fluctuations are maintained are thus favored. As a result, early structure formation is possible.
Since this thesis is mainly about a calculation in the MSSM, one should discuss the lightest neutralino as the WIMP suggested by this model. WIMPs are hypothetical particles which are massive and interact only by weak interaction and gravitation. Consequently, WIMPs are dark matter candidates.
Due to the earlier mentioned problems with neutrinos as candidates for dark matter, the Standard Model of particle physics does not offer a candidate for non-baryonic dark matter at all and needs an extension. As we will later discuss, the supersymmetry suggests superpartners for every particle of the SM and the Lightest Supersymmetric Particle

(LSP) is a well-motivated WIMP candidate.

3. WIMP relic density

Since WIMPs are possible dark matter candidates, it is useful to calculate the relic density of such particles in order to compare these results with experimentally established Dark Matter relic densities. The dark matter relic density $\Omega_c h^2 = 0.120 \pm 0.001$ in the Lambda Cold Dark Matter model (ΛCDM) was obtained by the *Planck* collaboration [Col+18] from *Planck* measurements of the Cosmic Microwave Background (CMB) where h describes the current Hubble expansion rate in units of $\mathrm{km\ s^{-1}\ Mpc^{-1}}$.
The idea is that the WIMP - in our case the lightest neutralino denoted by neutralino χ - existed in thermal equilibrium in the early universe until annihilation reactions which sustained the equilibrium "freezed out" and relic abundance remained. Annihilation reactions refer to the annihilations of neutralinos χ into particle-antiparticle pairs of lighter particles l ($\chi\chi \rightarrow l\bar{l}$) and vice versa ($l\bar{l} \rightarrow \chi\chi$). Neutralinos are Majorana particles so they are their own antiparticles. The Boltzmann equation (see eq. (3.1)[JKG96, p. 29]) is used here to describe quantitatively the time evolution of number density n for the neutralino. The derivation follows S. Dodelson[Dod03] and G. Jungman [JKG96]. The Hubble parameter is $h = \frac{\dot{a}}{a}$ wher a is the scale parameter of the universe and $< \sigma v >$ is the thermally averaged cross section for annihilations of the neutralino multiplied with the Møller velocity v.

$$\frac{dn}{dt} + 3nh =< \sigma v > \left((n_{\mathrm{EQ}})^2 - n^2 \right) \tag{3.1}$$

One has to consider that neutralinos are fermions so they obey the Fermi-Dirac distribution. Indeed, we are mostly interested in systems with temperatures smaller than $E - \mu$ so the Maxwell-Boltzmann statistics can be used to a good approximation. g indicates internal degrees of freedom of neutralinos. The number density of neutralinos

$$n = \frac{g}{(2\pi)^3} e^{\mu/T} \int e^{-E/T} d^3p, \tag{3.2}$$

is influenced by their chemical potential μ and its time dependence as well as the neutralino's mass m. Additionally, n_{χ}^{EQ} is the neutralino number density in equilibrium and is calculated by eq. (3.3)[Dod03, p. 61].

$$n_{\mathrm{EQ}} = \frac{g}{(2\pi)^3} \int e^{-E/T} d^3p = \begin{cases} g \left(\frac{mT}{2\pi}\right)^{3/2} e^{-m/T} & m >> T, \\ g \frac{T^3}{\pi^2} & m << T \end{cases} \tag{3.3}$$

Considering the case of the temperature T significantly dropping below the mass m, we see that number density n is decreasing exponentially (as long as the neutralinos are in equilibrium, see eq. (3.3)). Hereby, the annihilation rate $\Gamma =< \sigma v > \cdot n$ decreases as well and finally the annihilation rate is smaller than h. The annihilations of neutralinos stop and thus a relic density remains.
In the case of low temperatures in the late universe $m >> T$, the number density in equilibrium is suppressed by $e^{-m/T}$. Therefore, if the expansion of the universe was slow enough that $h < \Gamma$ until now, the existence of heavy neutralinos would be highly restrained due to neutralinos still being in equilibrium.
Looking at eq. (3.1) again, we notice that $-n^2 < \sigma v >$ accounts for annihilation of the neutralinos and $n_{\mathrm{EQ}}^2 < \sigma v >$ for the inverse reaction ergo the creation of them. Since creation and annihilation rates are equal in equilibrium

considering no number-violations[JKG96, p. 29], Boltzmann's equation simplifies to:

$$\frac{dn}{dt} + 3hn = 0 \tag{3.4}$$

$$\Leftrightarrow \frac{dn}{dt} = -3n\frac{1}{a}\frac{da}{dt} \tag{3.5}$$

$$\Rightarrow n \propto \frac{1}{a^3}. \tag{3.6}$$

Accordingly, in equilibrium the number density shrinks proportional to the expansion of space, in other words the comoving number density is constant.
In order to get some further estimates for the evolution of the number density, we utilize a slightly different form of eq. (3.1):

$$a^{-3}\frac{d(na^3)}{dt} =< \sigma v > \left((n_{\mathrm{EQ}})^2 - n^2\right). \tag{3.7}$$

Due to temperature scaling by $1/a$, we consider $(aT)^3$ to be time-independent and write

$$a^{-3}(Ta)^3\frac{d}{dt}\left(\frac{n}{T^3}\right) =< \sigma v > \left((n_{\mathrm{EQ}})^2 - n^2\right) \tag{3.8}$$

$$\Leftrightarrow \frac{dY}{dt} = T^{-3} < \sigma v > \left((n_{\mathrm{EQ}})^2 - n^2\right) \tag{3.9}$$

$$\Leftrightarrow \frac{dY}{dt} = T^3 < \sigma v > \left((Y_{\mathrm{EQ}})^2 - Y^2\right) \tag{3.10}$$

where $Y = n/T^3$ and $Y_{\mathrm{EQ}} = n_{\mathrm{EQ}}/T^3$. Furthermore, we introduce $x = m/T$ as a new time scale, because the relation between the mass of neutralino m and the temperature is characteristic for the number density n as we saw earlier. Considering $T \propto a^{-1}$, we see that $x \propto a$. As a result:

$$\frac{dx}{dt} = x \cdot \frac{\dot{a}}{a} = xh, \tag{3.11}$$

and we obtain:

$$hx\frac{dY}{dx} = T^3 < \sigma v > \left((Y_{\mathrm{EQ}})^2 - Y^2\right). \tag{3.12}$$

Following S. Dodelson [Dod03, p. 75], we write the Hubble parameter as $h(T = m) = h \cdot x^2$ because dark matter production takes place in the radiation era where the energy density is proportional to T^4. Using

$$\lambda = \frac{m^3 < \sigma v >}{h(m)} = \frac{xT^3 < \sigma v >}{h}, \tag{3.13}$$

as a scale for the ratio between the annihilation- and the Hubble-rate, we acquire:

$$\frac{dY}{dx} = \frac{\lambda}{x^2}\left((Y_{\mathrm{EQ}})^2 - Y^2\right). \tag{3.14}$$

Unfortunately, eq. (3.1) has no exact analytic solution. In general, $< \sigma v >$ is energy-dependent but we consider it to be energy-independent in order to obtain a rough analytic result for the final abundance $Y_\infty = Y(x >> 1)$. Since most physics happens at $x \sim 1$, where the left hand side of eq. (3.14) is of order Y and the right hand side of order $Y^2\lambda$, we demand that $Y = Y_{\mathrm{EQ}}$ as long as Y is not too small . This is because λ is very large and the terms on the right are therefore way stronger than the left hand side.
At later times after "freeze out" $x >> 1$, Y_{EQ} becomes quite small. Consequently, the neutralinos are no longer in

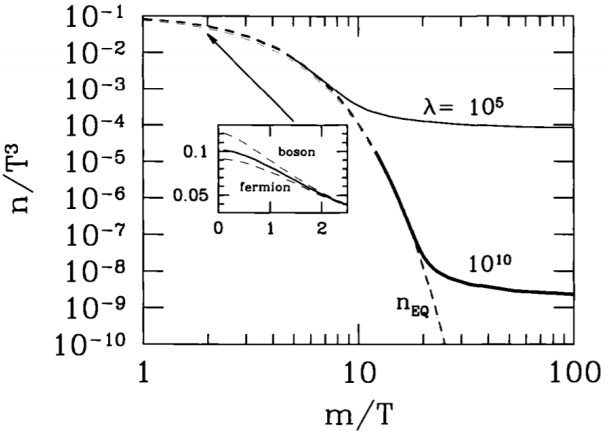

Figure 2: A numerical solution of the Boltzmann equation for different values of λ. Dashed lines show the number density in equilibrium and solid lines are the number densities after "freeze out". The enlagared image shows the difference between Maxwell-Boltzmann-statistics and quantum-statistics.[Dod03, p. 76]

equilibrium and we can write:

$$\frac{dY}{dx} \simeq -\frac{\lambda}{x^2}Y^2. \tag{3.15}$$

We integrate from time of "freeze out" x_f until late times $x = \infty$ and use that $Y(x_f)$ is vastly larger than Y_∞:

$$-\int_{Y(x_f)}^{Y_\infty} \frac{1}{Y^2}dY = \int_{x_f}^{\infty} \frac{\lambda}{x^2}dx \tag{3.16}$$

$$\Leftrightarrow \frac{1}{Y_\infty} - \frac{1}{Y(x_f)} = \frac{\lambda}{x_f} \tag{3.17}$$

$$\Rightarrow Y_\infty \approx \frac{x_f}{\lambda}. \tag{3.18}$$

Since eq. (3.18) is dependent on the temperature x_f of "freeze out", this is not a full result. We use a rough order-of-magnitude estimation $x_f \sim 10$[Dod03, p. 75] though to finish the calculation.
Lastly, we have to consider that neutralino density falls of with a^{-3} after "freeze out". Therefore, today's energy density ρ of neutralinos is calculated by

$$\rho = mY_\infty \left(\frac{a_c T_c}{a_{\text{today}} T_{\text{today}}}\right)^3, \tag{3.19}$$

where a_c is the scale factor right after Y_∞ is roughly reached and T_c is the relating temperature. It is important to note that aT is not constant during expansion of the universe due to the fact that universe is heated by the annihilation of massive particles. Consequently, T does not exactly fall with a^{-1}. According to Dodelson $\left(\frac{a_c T_c}{a_{\text{today}} T_{\text{today}}}\right)^3 \simeq \frac{1}{30}$ and we obtain:

$$\rho = mY_\infty \frac{1}{30}. \tag{3.20}$$

Finally, we obtain an expression for today's density Ω_χ of neutralinos by dividing eq. (3.20) through the critical density ρ_{cr} :

$$\Omega_\chi = \frac{mY_\infty}{30\rho_{cr}}. \tag{3.21}$$

By determining $h(m)$, doing further calculations and inserting our rough estimate for Y_∞, we obtain that Ω_χ is mostly dependent from the cross section $< \sigma v >$. The mass of the neutralino does not have a huge impact on its relic density. Ω_χ is compared with the experimental results for dark matter density of $\simeq 0.3$. S. Dodelson concludes that cross

sections in the order of $10^{-19}\mathrm{cm}^2$ are giving realistic relic density while neutralino's cross section might be of the same magnitude.
In fig. 2, we show the numerical solution to eq. (3.14). One notices that comoving number density attains a constant value relatively short after the annihilations "freeze out" and neutralinos or thermal WIMP's in general are no longer in equilibrium. Additionally for larger ratios λ, the "freeze out" occurs later and consequently the relic density is lower. Furthermore, the approximation of neglecting +1 in denominator of Fermi-Dirac-statistics seems appropriate since there is only a noticeable difference for $x < 1$.
If there are sparticles with only a small difference in mass to the lightest neutralino, their annihilation and co-annihilation processes are no longer suppressed and need to be considered for the calculation of relic density. Accordingly, the Boltzmann equation eq. (3.1) does not contain the whole information and needs to be extended. The annihilations are described by replacing $< \sigma v >$ through

$$< \sigma_{\mathrm{ann}} v >= \sum_{i,j} < \sigma_{ij} v_{ij} > \frac{n_{i,\mathrm{EQ}}}{n_{\mathrm{EQ}}} \frac{n_{j,\mathrm{EQ}}}{n_{\mathrm{EQ}}}, \tag{3.22}$$

with sum over i, j running over all supersymmetric particles (sparticles) and their number densities in equilibrium $n_{i,\mathrm{EQ}}$ [Sch+19]. σ_{ij} corresponds to the annihilation cross section of sparticles i and j. Accordingly, v_{ij} is the Møller velocity of these annihilating sparticles. As a result, coupled differential equations need to be solved. The suppression of annihilations and co-annihilations of sparticles with much larger mass than neutralino's mass m is described by the fact that number densities in equilibrium are related by

$$\frac{n_{i,\mathrm{EQ}}}{n_{\mathrm{EQ}}} \sim \exp\left(-\frac{m_i - m}{T}\right), \tag{3.23}$$

where m_i is the mass of sparticle i.
The MSSM allows a theoretical prediction of dark matter relic density. By comparing this with the experimental data, one is able to identify favored regions of parameter space.

4. Introduction into the Minimal Supersymmetric Standard Model

Although the Standard Model provides an excellent description of accelerator experiments, it is obvious that there might be new physics in 16 order of magnitudes between the reduced Planck scale of $\sim 10^{18}\mathrm{GeV}$ where quantum-gravitational effects are expected and some $100\,\mathrm{GeV}$ achievable in accelerators. As previously discussed, strong evidence suggests the existence of non-baryonic dark matter as part of physics beyond the Standard Model. There are different reasons to demand a supersymmetry as part of new physics but probably the strongest one is the solution of the hierarchy problem, whereas this was not the initial reason for the development of such theories. For a more detailed introduction into supersymmetry see "A Supersymmetry Primer" by S. Martin[MAR98].
The Higgs mechanism introduced the Higgs field in order to spontaneously break the electroweak $SU(2)_L \times SU(1)_Y$ symmetry and to allow masses of gauge bosons $W^{\pm}$ and Z^0 in the order of $100\,\mathrm{GeV}$. Because of that, the mass of corresponding scalar Higgs boson m_H was predicted to be in the order of $100\,\mathrm{GeV}$ as well[MAR98, p. 3] while experiments at LHC measured it to be $125\,\mathrm{GeV}$.
The Higgs potential is extremely sensitive to the existence of heavier particles. This means that the mass m_H gets radiative corrections by virtual effects of every particle which couples directly or indirectly to the Higgs field.
For example, if a Dirac fermion f of mass m_f couples to the Higgs field with a term $-\lambda_f H \bar{f} f$ in the Lagrangian, m_H

Figure 3: Corrections to Higgs (mass)².

receives a correction through the Feynman diagram in fig. 3a of

$$\Delta m_H^2 = \frac{|\lambda_f|^2}{16\pi^2}\left(-2\Lambda_{UV}^2 + 6m_f^2 \ln\left(\Lambda_{UV}/m_f\right) + ...\right), \tag{4.1}$$

where Λ_{UV} is an ultraviolet momentum cutoff[MAR98, p. 3]. Λ_{UV} is utilized for regulation of the loop integrals and can be taken as the energy scale where the new physics enters and modifies the theory. The problem arises that if Λ_{UV} is of same order as the Planck scale, the corrections to m_H are getting extremely large.
Besides these corrections, the other Standard Model particles do not have corrections with quadratic dependence to Λ_{UV} but quarks, leptons and electroweak gauge bosons owe their masses to vacuum expectation value of the Higgs field. Therefore, the whole mass spectrum of Standard Model is dependent on Λ_{UV}.
Furthermore, one can look at the radiative corrections of m_H caused by a massive complex scalar S of mass m_S. Supposing S couples to the Higgs field with a term $-\lambda_S|H|^2|S|^2$, then the loop in fig. 3b yields a correction [MAR98, p. 4]

$$\Delta m_H^2 = \frac{\lambda_S}{16\pi^2}\left(\Lambda_{UV}^2 - 2m_S^2 \ln\left(\Lambda_{UV}/m_S\right) + ...\right). \tag{4.2}$$

Considering the contributions to Δm_H^2, we notice the relative minus sign between fermion and boson loop corrections to m_H and see that a symmetry - called *supersymmetry* - could regulate the corrections through relating bosonic and fermionic state. Regarding to low-energy supersymmetry, in fact, the momentum integrals of perturbation theory are softened so that the quadratic dependence on energy scales much larger than the electroweak scale are reduced to at most a logarithmic dependence[JKG96, p. 42]. Therefore, the hierarchy between the electroweak scale and Planck-scale would be conserved by existence of low-energy supersymmetry without fine-tuning the couplings.
Leaving the fact aside that this was just a rough explanation of the hierarchy problem, it should provide a motivation for building a supersymmetric model.

4.1. Idea of supersymmetry

Supersymmetric theories consist in the simplest case of chiral supermultiplets (a two-component Weyl fermion and a complex scalar field) and gauge supermultiplets (spin-1 gauge bosons and spin$-1/2$ gauginos, both massless and having two helicity states) where numbers of bosonic and fermionic degrees of freedom are equal. The fermion and boson states are known as *superpartners* of each other and have the same electric charges, weak isospin and color degrees of freedom. A supersymmetry transformation between those superpartner states is described schematically by the operator Q (in general, the states are transformed up to spacetime translations or rotations by a combination of Q and $Q^\dagger$):

$$Q\,|\text{Boson}\rangle = |\text{Fermion}\rangle\,, \quad Q\,|\text{Fermion}\rangle = |\text{Boson}\rangle\,. \tag{4.3}$$

Q must be an anticommuting spinor, which are complex objects so the hermitian conjugate $Q^\dagger$ has to be a symmetry generator too. Because these operators are fermionic and carry the spin $1/2$, supersymmetry must be a spacetime

symmetry. Accordingly, it can be shown that Q and $Q^\dagger$ must satisfy the schematic relations:

$$\{Q, Q^\dagger\} = P^\mu, \tag{4.4}$$

$$\{Q, Q\} = \{Q^\dagger, Q^\dagger\} = 0, \tag{4.5}$$

$$[P^\mu, Q] = [P^\mu, Q^\dagger] = 0, \tag{4.6}$$

where P^μ is the momentum generator of spacetime translations. Due to commuting with P^μ, the operators Q and $Q^\dagger$ must commute with the (mass)^2 operator $-P^2$ as well. Objects of one supermultiplet thus must have the same eigenvalues $-P^2$ which means the same masses[MAR98, p. 5]. Consequently, it would have been easy to observe many supersymmetric particles in experiments for a long time. Since no supersymmetric particles have been detected yet, supersymmetry must be broken in the vacuum state in order to provide different masses. For maintaining supersymmetry as a solution to the hierarchy problem, one considers "soft" supersymmetry breaking where the effective Lagrangian

$$\mathscr{L} = \mathscr{L}_{\text{SUSY}} + \mathscr{L}_{\text{soft}} \tag{4.7}$$

is built by the term $\mathscr{L}_{\text{SUSY}}$ preserving invariance under supersymmetry transformations and the supersymmetry-breaking part $\mathscr{L}_{\text{soft}}$ containing only mass terms and couplings of positive mass dimension. The superpartner's masses can not be too heavy compared to the electroweak breaking scale due to radiative corrections of the Higgs mass by mass terms in $\mathscr{L}_{\text{soft}}$, otherwise the Higgs vacuum expectation value could not provide the detected masses of $W^\pm$ and Z^0. As a result, the masses of the lightest superpartners must not be much larger than $1\,\text{Tev}$ in order to solve the hierarchy problem by SUSY [MAR98, p. 10-11].

4.2. Minimal Supersymmetric Standard Model

The Minimal Supersymmetric Standard Model is built up by chiral and gauge supermultiplets where every particle of the Standard Model is in either a gauge or chiral supermultiplet together with a superpartner. The superpartners' spin differs by $1/2$. Since all fermions of the SM are transforming differently under the gauge group depending on if they are left- or right-handed, all of these fermions need to be part of a chiral supermultiplet and have a scalar superpartner. This is because the fermionic members of gauge supermultiplets need to transform as left- and right-handed particles equally under the gauge group due to properties of gauge bosons. Partners of quarks and leptons thus have spin-0 and are called *squarks* and *sleptons*. Particularly, the names of all superpartners of quarks and leptons are made by putting an "s" to the front.

Left- and right-handed quarks and leptons have their own complex scalar superpartners and are part of an own chiral supermultiplet. The symbols of supersymmetric partners are equal to the particles of the Standard Model except for a tilde. The superpartner of a left-handed electron is a selectron $\tilde{e}_L$ where the L does not refer to an actual handedness (since $\tilde{e}_L$ has spin-0) but to the handedness of the Standard Model partner. The gauge interactions are similar for the two members of a supermultiplet.

Since right-handed neutrinos do not exist according to the Standard Model, the subscript L can be dropped and e, μ and τ are used to note their lepton flavor: $\tilde{\nu}_e, \tilde{\nu}_\mu, \tilde{\nu}_\tau$.

Besides this, the Higgs boson is a scalar and is therefore part of a chiral supermultiplet, but only one Higgs chiral supermultiplet is not enough to construct a consistent quantum theory. This is because the electroweak symmetry would receive an anomaly due to the fermionic partner of the Higgs boson having either weak hypercharge $Y = 1/2$ or $Y = -1/2$. Supposing there would be two Higgs supermultiplets where one has $Y = 1/2$ and the other $Y = -1/2$ with each containing a weak isodoublet of fermions, the anomaly cancels out.

Additionally, in supersymmetric theories only $Y = 1/2$ Higgs supermultiplets have the Yukawa couplings needed in

Table 1: Chiral supermultiplets of MSSM categorized by transformation properties under $SU(3)_C \times SU(2)_L \times U(1)_Y$ [MAR98, p. 8]

Names		spin 0	spin 1/2	$SU(3)_C$, $SU(2)_L$, $U(1)_Y$
squarks, quarks	Q	$(\tilde{u}_L \;\; \tilde{d}_L)$	$(u_L \;\; d_L)$	$(\mathbf{3}, \mathbf{2}, \frac{1}{6})$
($\times$3 families)	$\overline{u}$	$\tilde{u}_R^*$	$u_R^\dagger$	$(\overline{\mathbf{3}}, \mathbf{1}, -\frac{2}{3})$
	$\overline{d}$	$\tilde{d}_R^*$	$d_R^\dagger$	$(\overline{\mathbf{3}}, \mathbf{1}, \frac{1}{3})$
sleptons, leptons	L	$(\tilde{\nu} \;\; \tilde{e}_L)$	$(\nu \;\; e_L)$	$(\mathbf{1}, \mathbf{2}, -\frac{1}{2})$
($\times$3 families)	$\overline{e}$	$\tilde{e}_R^*$	$e_R^\dagger$	$(\mathbf{1}, \mathbf{1}, 1)$
Higgs, higgsinos	H_u	$(H_u^+ \;\; H_u^0)$	$(\tilde{H}_u^+ \;\; \tilde{H}_u^0)$	$(\mathbf{1}, \mathbf{2}, +\frac{1}{2})$
	H_d	$(H_d^0 \;\; H_d^-)$	$(\tilde{H}_d^0 \;\; \tilde{H}_d^-)$	$(\mathbf{1}, \mathbf{2}, -\frac{1}{2})$

Table 2: Gauge supermultiplets of MSSM categorized by transformation properties under $SU(3)_C \times SU(2)_L \times U(1)_Y$ [MAR98, p. 9]

Names	spin 1/2	spin 1	$SU(3)_C$, $SU(2)_L$, $U(1)_Y$
gluino, gluon	$\tilde{g}$	g	$(\mathbf{8}, \mathbf{1}, 0)$
winos, W bosons	$\widetilde{W}^\pm \;\; \widetilde{W}^0$	$W^\pm \;\; W^0$	$(\mathbf{1}, \mathbf{3}, 0)$
bino, B boson	$\tilde{B}^0$	B^0	$(\mathbf{1}, \mathbf{1}, 0)$

order to give up-type quarks of electric charge +2/3 their mass. Whereas, Higgs supermultiplets of hypercharge $Y = -1/2$ give down-type quarks their mass. Ergo, the Higgs bosons are indicated by an index u or d according to their hypercharge $Y = \pm 1/2$. The members of an isodoublets have a third component of isospin $I_3 = +1/2$ or $I_3 = -1/2$. As a result, the electric charges of the members of the isodoublet with $Y = +1/2$ have electrical charge $Q = Y + I_3$ of +1 or 0. Analogously, for $Y = -1/2$ it gives the electrical charges 0 or −1. This leads to the notation for the members of these doublets to H_u^+, H_u^0 and H_d^0, H_d^- with neutral Higgs boson of SM being a linear combination of H_u^0 and H_d^0.

In general, names of spin-1/2 superpartners are constructed by attaching "-ino" to the Standard Model name. Hence, superpartners of Higgs bosons are called higgsinos. The chiral supermultiplets are presented in table 1 and categorized by their properties under the Standard Mode gauge transformation where u_L and d_L as well as e_L and ν_e build isodoublets. Since the convention of chiral supermultiplets defined for left-handed Weyl-fermions is used, the conjugates of right-handed quarks, leptons and their superpartners are displayed. Vector bosons of the Standard Model are part of gauge supermultiplets so their superpartners have spin-1/2 and are called gauginos (see table 2). The superpartner of the gluon g is the gluino $\tilde{g}$ and the superpartners of W bosons and the B boson are called winos and bino. Since W^0 and B^0 mix after electroweak symmetry breaking to Z^0 and γ, the analogue gaugino mixing states are called $\tilde{Z}^0$ and $\tilde{\gamma}$[MAR98, p. 7-10].

After electroweak symmetry breaking and taking into account the supersymmetry breaking, the superpartners do not necessarily provide the mass eigenstates of the particles. This is because particles of the same quantum numbers mix. This occurs for sets of squarks, sleptons and Higgs scalars of the same charge. For instance, the mass eigenstates of stop are $\tilde{t}_1$ and $\tilde{t}_2$ which are mixing states of $\tilde{t}_L$ and $\tilde{t}_R$. Analogously, the electroweak gauginos and the higgsinos mix. This leads to the neutralinos χ which are mixing states of $\tilde{W}^0$, $\tilde{B}^0$ and the neutral higgsinos. The lightest neutralino serves as a WIMP candidate due to the conservation of R-parity.

A new symmetry called "R-parity" is introduced to the MSSM as a multiplicative conserved quantum number with

$$P_R = (-1)^{3(B-L)+2s}, \tag{4.8}$$

where s is the particles spin, B the baryon number and L its lepton number. Consequently, all particles of Standard Model and the Higgs bosons have R-parity +1 and their superpartners −1. The MSSM is defined to conserve R-parity in order to conserve B and L due to proton decay not being observed in experiments. The Standard Model does not allow B or L violating terms. In contrast, such terms in superpotentials of MSSM are gauge-invariant and renormalizable but are not included. The postulate of exact conserved R-parity allows the existence of the stable LSP as a dark matter candidate since such LSP has $P_R = -1$ (odd R-parity) and is only able to annihilate with another supersymmetric particle into Standard Model particles of even R-parity $P_R = 1$. Accordingly, the lightest neutralino as an only weakly and gravitational interacting particle serves as a candidate for a WIMP in MSSM. Moreover, all sparticles decay eventually into a state including an odd number of LSPs. Additionally, sparticles can only be produced in even numbers in particle colliders. [MAR98, p. 34-36]

5. Analytic calculation of gluino stop co-annihilation into top gluon

Our target is to evaluate the cross section for the co-annihilation of a gluino $\tilde{g}$ with a stop $\tilde{t}_1$ into a top-quark and a gluon. The differential cross section $d\sigma$ is given by eq. (5.2) [HM84, p. 90] with incident flux

$$F = 4(p_A \cdot p_B)^2 - m_{\tilde{g}}^2 m_{\tilde{t}_1}^2, \tag{5.1}$$

where p_A and p_B are the four-momenta of gluino and stop respectively. m_i indicates the mass of particle i.

$$d\sigma = \frac{|M|^2}{F} dQ \tag{5.2}$$

The phase space factor is given by

$$dQ = (2\pi)^4 \delta^{(4)}(k_1 + k_2 - p_A - p_B) \frac{d^3k_1}{(2\pi)^3 2E_t} \frac{d^3k_2}{(2\pi)^3 2E_g}, \tag{5.3}$$

with the four-momenta k_1 of top-quark and k_2 of gluino. E_i is the energy of particle i.
Furthermore, in the center-of mass frame this equation can be simplified and leads to the differential cross section

$$\frac{d\sigma}{d\Omega} = \frac{1}{64\pi^2 s} \frac{p_f}{p_{\text{cm}}} |M|^2 \tag{5.4}$$

with $p_f = |\vec{k}_1| = |\vec{k}_2|$, $p_{\text{cm}} = |\vec{p}_A| = |\vec{p}_B|$, solid angle element $d\Omega$ about $\vec{k}_1$ and the mandelstam variable $s = (E_t + E_g)^2$.
The integration over element of solid angle $d\Omega$ thus leads to the total cross section.
Accordingly, the whole physics are defined by invariant amplitude M. Firstly, we need to figure out which Feynman diagrams are relevant in the lowest order of perturbation theory for the process we want to examine. Afterwards, we use the Feynman rules in appendix A to establish the squared invariant amplitude $|M|^2$ by making use of the trace theorems in appendix B.1 and are able to calculate the cross section in the lowest order (tree level).

5.1. Feynman diagrams

At first, we are searching for s-channel diagrams. Gluino and stop are coming in and couple to the propagator. In order to conserve R-parity, only a standard model particle can be produced since we are considering the lowest order processes. Due to electric charge conservation, the propagator must be a particle of charge +2/3. Since the total topness of incoming and outgoing particles are both 1, the propagator of s-channel has to be of topness 1, too. Considering R-parity, charge conservation and flavor conservation, one knows that the propagator of the s-channel has to be a top-quark. Putting this together, we can construct the Feynman diagram for the s-channel (see fig. 4). One is able to construct invariant amplitude M_s for diagram in fig. 4 using the Feynman rules. We start establishing

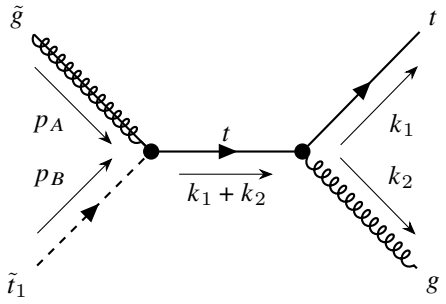

Figure 4: S-channel Feynman diagram for gluino stop co-annihilation in lowest order.

$-iM_S$ in eq. (5.5) by writing the factor of outgoing external fermion line or incoming antifermion line to the front. We consider the majorana gluino to be an incoming fermion. That is why we start with the spinor $\bar{u}^{(s_1)}(k_1)$ for the outgoing top-quark. Additionally, the factor for an outgoing gluon of mass 0 has to be multiplied which is the polarization vector $\epsilon^{*\mu}(k_2)$. Following the fermion chain, we have to multiply the vertex factor for quark-gluon coupling (see eq. (A.1)). k is the color index of outgoing top quark, j the index of the propagating top quark and a indicates the color of outgoing gluon. Moreover, we have to continue with the propagator for a top-quark of momentum $k_1 + k_2$. Since the top quark is a spin 1/2 particle of mass m_t, the propagator can be written as:

$$\frac{i(\not{k}_1 + \not{k}_2 + m_t)}{(k_1 + k_2)^2 - m_t^2 + i\epsilon}\delta_{jl},$$

where j and l are the color of the propagator at the vertices. To continue, one has to include the vertex factor for squark-gluino-quark coupling (see eq. (A.3)) where i is the color index of scalar top and b the one of gluino. We complete $-iM_s$ by the factor for an incoming gluino of momentum p_A which is $u(p_A, m_{\tilde{g}})$ and the factor 1 for the scalar stop. Hence, we receive eq. (5.5) for the invariant amplitude of s-channel.

$$\begin{aligned} -iM_s =& \bar{u}^{(s_1)}(k_1)\varepsilon^{*\mu}(k_2)\left(-ig_s T^a_{kj}\gamma_\mu\right)\left(\frac{i(\not{k}_1 + \not{k}_2 + m_t)}{(k_1 + k_2)^2 - m_t^2 + i\epsilon}\delta_{jl}\right) \\ & \left(-i\sqrt{2}g_s T^b_{li}(R_{1L}P_R - R_{1R}P_L)\right)u^{(s_2)}(p_A) \end{aligned} \tag{5.5}$$

Furthermore, we need to figure out the other possible diagrams at tree level. For the t-channel, one notices that the propagator needs to be either top or stop considering electric charge conservation and topness conservation. The conservation of R-parity at the vertices ensures the propagator to be a supersymmetric particle with odd R-parity ($P_R = -1$). As a result, a scalar top is the propagator in the t-channel. Since there are no couplings between $\tilde{q}_1$,$\tilde{q}_2$ and g, the propagator is a $\tilde{t}_1$ too. We show the Feynman diagram for t-channel in fig. 5 .
Analogue to $-iM_s$, we can write $-iM_t$ using the Feynman rules. Firstly, the factor for outgoing t is written to the front and is multiplied by the vertex factor for quark-squark-gluino coupling (see eq. (A.2)). Then, we follow the

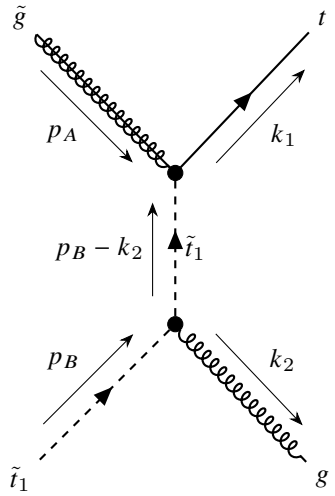

Figure 5: T-channel Feynman diagram for gluino stop co-annihilation in lowest order.

fermion line and multiply the factor for an external gluino. Afterwards, the propagator of a scalar top with momentum $k_1 - p_A$, mass $m_{\tilde{t}_1}$ and colors h and l at the vertices is considered. The propagator can be written as:

$$\frac{i}{(k_1 - p_A)^2 - m_{\tilde{t}_1}^2 + i\epsilon}\delta_{hl}.$$

To complete $-iM_t$, the polarization vector for the external gluon and the factor for squark-gluon coupling (see eq. (A.4)) need to be appended.

$$\begin{aligned} -iM_t =& \bar{u}^{(s_1)}(k_1)\left(-i\sqrt{2}\mathrm{g_s}T^b_{kh}(R_{1L}P_R - R_{1R}P_L)\right)u^{(s_2)}(p_A) \\ & \left(\frac{i}{(k_1 - p_A)^2 - m_{\tilde{t}_1}^2 + i\epsilon}\delta_{hl}\right)\varepsilon^{*\mu}(k_2)\left(-i\mathrm{g_s}T^a_{li}(2p_B - k_2)_\mu\right) \end{aligned} \tag{5.6}$$

Finally, we try to find a propagator for the u-channel diagram. The propagator should have a topness of 0 since it couples to stop and top. Furthermore, the propagator has to be of electric charge 0 since gluino and gluon have no electric charge but top and stop both are of electric charge $2/3$ due to being superpartners. In the end, conservation of R-Parity forces the propagator to be a gluino. The Feynman diagram for u-channel can be seen in fig. 6.
In use of the Feynman rules, the amplitude $-iM_u$ is given in in eq. (5.7). Looking at eq. (5.7), we start at the outgoing

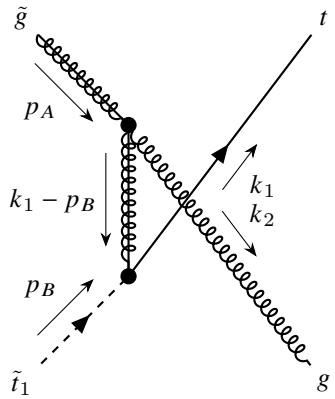

Figure 6: U-channel Feynman diagram for gluino stop co-annihilation in lowest order.

fermion, write the spinor $\bar{u}^{(s_1)}(k_1)$ to the front and multiply 1 for the scalar top. To continue, the vertex factor for quark-squark-gluino coupling eq. (A.2) is appended analogue to establishing the previous amplitudes. Due to gluino being a spin 1/2 fermion of mass $m_{\tilde{g}}$, we write for the gluino propagator with momentum $k_1 - p_B$ and colors c respectively d at the vertices:

$$\frac{i(\not{k}_1 - \not{p}_B + m_{\tilde{g}})}{(k_1 - p_B)^2 - m_{\tilde{g}}^2}\delta^{cd}.$$

Finally, we multiply the vertex factor of gluino-gluon coupling (see eq. (A.5)) and factors for an external gluino and gluon.

$$\begin{aligned} -iM_u =& \bar{u}^{(s_1)}(k_1)\left(-i\sqrt{2}\mathrm{g_s}T^d_{ki}(R_{1L}P_R - R_{1R}P_L)\right) \\ & \left(\frac{i(\not{k}_1 - \not{p}_B + m_{\tilde{g}})}{(k_1 - p_B)^2 - m_{\tilde{g}}^2 + i\epsilon}\delta^{cd}\right)\left(-\mathrm{g_s}f^{acb}\gamma_\mu\right)u^{(s_2)}(p_A)\varepsilon^{*\mu}(k_2) \end{aligned} \tag{5.7}$$

Consequently, the invariant Mandelstam-Variables for these diagrams are:

$$s = (k_1 + k_2)^2 = (p_A + p_B)^2, \tag{5.8}$$

$$t = (k_1 - p_A)^2 = (k_2 - p_B)^2, \tag{5.9}$$

$$u = (k_2 - p_A)^2 = (k_1 - p_B)^2. \tag{5.10}$$

Since $\varepsilon^{*\mu}$ represents one component of a polarization vector, it is a scalar and can be shifted to the head of the amplitudes. Analogously, T^a_{kj}-like objects are matrix elements so they can be placed there, too. Additionally, the offset $i\epsilon$ can be neglected since the poles are neglectable in this process. Placing the scalars at the front, inserting the Mandelstam-variables and evaluating the Kronecker deltas gives:

$$M_s = \frac{\sqrt{2}\mathrm{g_s}^2T^a_{kj}T^b_{ji}\varepsilon^{*\mu}(k_2)}{s - m_t^2}\bar{u}^{(s_1)}(k_1)\gamma_\mu\left(\not{k}_1 + \not{k}_2 + m_t\right)\left(R_{1L}P_R - R_{1R}P_L\right)u^{(s_2)}(p_A), \tag{5.11}$$

$$M_t = \frac{\sqrt{2}\mathrm{g_s}^2T^b_{kl}T^a_{li}\varepsilon^{*\mu}(k_2)}{t - m_{\tilde{t}_1}^2}\bar{u}^{(s_1)}(k_1)\left(R_{1L}P_R - R_{1R}P_L\right)u^{(s_2)}(p_A)(2p_B - k_2)_\mu, \tag{5.12}$$

$$M_u = \frac{-i\sqrt{2}\mathrm{g_s}^2T^c_{ki}f^{acb}\varepsilon^{*\mu}(k_2)}{u - m_{\tilde{g}}^2}\bar{u}^{(s_1)}(k_1)\left(R_{1L}P_R - R_{1R}P_L\right)\left(\not{k}_1 - \not{p}_B + m_{\tilde{g}}\right)\gamma_\mu u^{(s_2)}(p_A). \tag{5.13}$$

$R_{1L} = \cos\theta_{\tilde{t}}$ and $R_{1R} = \sin\theta_{\tilde{t}}$ are elements of the mixing matrix for scalar tops. Because of having left-handed and right-handed top-quarks, there are also two scalar top eigenstates. Scalar tops have the same quantum numbers and are thus able to mix their states. This means that the superpartners of left-handed and right-handed tops are not necessarily the mass eigenstates of scalar tops.

5.2. Evaluation of squared amplitudes

After establishing the lowest-order amplitude of the three possible diagrams it is necessary to determine the total squared amplitude $|M|^2$. We are interested in developing a cross section which allows scattering in every possible spin-, color- and polarization-configuration because these information are not detected in experiments. Hence, we need to sum over the spins, polarizations and colors of the outgoing particles and average over analogue sums for incoming particles. This is expressed by $\overline{|M|^2}$. The averaging factors will be included in the end because they are

equal for each term.
Because of having three amplitudes M_s, M_t and M_u, which add up to the total amplitude, the calculation of $\overline{|M|^2}$ leads to:

$$\begin{aligned}\overline{|M|^2} =& \sum_{\text{spin,col.,pol.}} (M_s + M_t + M_u)(M_s + M_t + M_u)^\dagger \\ =& \sum_{\text{spin,col.,pol.}} \{M_s M_s^\dagger + M_t M_t^\dagger + M_u M_u^\dagger + 2\text{Re}(M_s M_t^\dagger) + 2\text{Re}(M_t M_u^\dagger) + 2\text{Re}(M_u M_s^\dagger)\} \\ =& \overline{|M_s^2|} + \overline{|M_t^2|} + \overline{|M_u^2|} + 2\text{Re}(\overline{M_s M_t^\dagger}) + 2\text{Re}(\overline{M_t M_u^\dagger}) + 2\text{Re}(\overline{M_u M_s^\dagger}).\end{aligned} \tag{5.14}$$

Equation (5.14) is obtained by using that $M_i M_j^\dagger$ with $i \neq j$, $(i, j = u, s, t)$ is a scalar and therefore:

$$M_i M_j^\dagger + M_j M_i^\dagger = M_i M_j^\dagger + c.c. = 2\text{Re}(M_i M_j^\dagger) \tag{5.15}$$

When calculating the squared amplitudes, it appears that the calculation can be split into a color part $|M_{\text{color}}|^2$ and a Dirac-part containing Dirac matrices γ^μ and spinors $|M_{\text{dirac}}|^2$. This means that the summation over colors can be evaluated separately from the summation over polarization and spins:

$$\overline{|M|^2} = \sum_{\text{spin,col.,pol.}} |M|^2 = \sum_{\text{spin,col.,pol.}} |M_{\text{color}}|^2 |M_{\text{dirac}}|^2 = \sum_{\text{col.}} |M_{\text{color}}|^2 \sum_{\text{spin,pol.}} |M_{\text{dirac}}|^2. \tag{5.16}$$

5.2.1. Hermitian conjugation of amplitudes

First, it is required to identify the hermitian conjugation of the three M_i. Then six terms need to be evaluated.
Starting with the hermitian conjugation of M_s(eq. (5.11)), we use the definition of a "barred" spinor $\bar{u} = u\gamma^0$. The scalars need to be complex conjugated and can be shifted to the front. Spinors and matrices need to be reversed in order and each hermitian conjugated. Furthermore, one can make use of the general hermitian conjugation for γ-matrices (see eq. (B.2)) and the fact that the chirality operators and γ^0 are hermitian. We are using the Feynman-slash notation and that momentum components like k_1^μ are real scalars. Therefore, the hermitian conjugation of a slashed momentum gives a multiplication with γ^0 from left and right. We obtain by using $m_t = \gamma^0 m_t \gamma^0$:

$$M_s^\dagger = \frac{\sqrt{2}\text{g}_\text{s}^2 T_{kj}^{*a} T_{ji}^{*b} \varepsilon^\mu(k_2)}{s - m_t^2} u^{\dagger(s_2)}(p_A)(\cos\theta_{\tilde{t}} P_R - \sin\theta_{\tilde{t}} P_L)\gamma^0 \left(\not{k}_1 + \not{k}_2 + m_t\right) \gamma^0\gamma^0\gamma_\mu\gamma^0\gamma^0 u^{(s_1)}(k_1) \tag{5.17}$$

In consideration of μ being a dummy index, where a summation over μ is intended, one changes μ to ν. We will multiply the hermitian conjugated amplitudes with the amplitudes and need to be able to distinguish between the dummy indices. Analogously, the color j is replaced by h. Due to T-matrices being hermitian (see eq. (B.24)), T_{kh}^{*a} can be expressed by T_{hk}^a and T_{hi}^{*b} by T_{ih}^b as well. The products $\gamma^0 \cdot \gamma^0$ can be dropped since they result in identity matrices. Lastly, the remaining γ^0 can be shifted by $(\cos\theta_{\tilde{t}} P_R - \sin\theta_{\tilde{t}} P_L)$, taking into account the anti-commutation of γ^5 and γ^0, in order to use $u^{\dagger(s_2)}(p_A)\gamma^0 = \bar{u}^{(s_2)}(p_A)$ again:

$$M_s^\dagger = \frac{\sqrt{2}\text{g}_\text{s}^2 T_{hk}^a T_{ih}^b \varepsilon^\nu(k_2)}{s - m_t^2} \bar{u}^{(s_2)}(p_A)(\cos\theta_{\tilde{t}} P_L - \sin\theta_{\tilde{t}} P_R) \left(\not{k}_1 + \not{k}_2 + m_t\right) \gamma_\nu u^{(s_1)}(k_1). \tag{5.18}$$

Analoguesly, one can write for $M_t^\dagger$:

$$M_t^\dagger = \frac{\sqrt{2}\mathrm{g_s}^2 T^b_{hk} T^a_{ih} \varepsilon^\nu(k_2)}{t - m^2_{\tilde{t}_1}} (2p_B - k_2)_\nu \bar{u}^{(s_2)}(p_A)(\cos\theta_{\tilde{t}} P_L - \sin\theta_{\tilde{t}} P_R) u^{(s_1)}(k_1). \tag{5.19}$$

Due to structure constants f^{acb} being real, we similarly obtain for the hermitian conjugation of eq. (5.13):

$$M_u^\dagger = \frac{+i\sqrt{2}\mathrm{g_s}^2 T^d_{ik} f^{adb} \varepsilon^\nu(k_2)}{u - m^2_{\tilde{g}}} \bar{u}^{(s_2)}(p_A)\gamma_\nu(\not{k}_1 - \not{p}_B + m_{\tilde{g}})(\cos\theta_{\tilde{t}} P_L - \sin\theta_{\tilde{t}} P_R) u^{(s_1)}(k_1). \tag{5.20}$$

5.2.2. Squared invariant amplitude of s-channel

Starting with calculating $\overline{|M_s^2|}$, we need to sum over the spins s_1 and s_2 of the external top-quark and gluino, colors i, k, a, b of external color-charged particles and the polarization of the external gluon.

$$\begin{aligned}\sum_{\text{spin,col.,pol.}} M_s M_s^\dagger = \sum_{i,k,a,b,s1,s2,\lambda} & \frac{\sqrt{2}\mathrm{g_s}^2 T^a_{kj} T^b_{ji} \varepsilon^{*\mu(\lambda)}(k_2)}{s - m_t^2} \bar{u}^{(s_1)}(k_1)\gamma_\mu\,(\not{k}_1 + \not{k}_2 + m_t)\,(\cos\theta_{\tilde{t}} P_L - \sin\theta_{\tilde{t}} P_R) u^{(s_2)}(p_A) \\ & \frac{\sqrt{2}\mathrm{g_s}^2 T^a_{hk} T^b_{ih} \varepsilon^{\nu(\lambda)}(k_2)}{s - m_t^2} \bar{u}^{(s_2)}(p_A)(\cos\theta_{\tilde{t}} P_L - \sin\theta_{\tilde{t}} P_R)\,(\not{k}_1 + \not{k}_2 + m_t)\,\gamma_\nu u^{(s_1)}(k_1).\end{aligned} \tag{5.21}$$

The fractions are scalars and we can simplify:

$$\begin{aligned}\overline{|M_s|^2} = & \sum_{i,k,a,b,s1,s2,\lambda} \frac{2\mathrm{g_s}^4 T^a_{kj} T^b_{ji} T^b_{ih} T^a_{hk}}{(s - m_t^2)^2} \varepsilon^{*\mu(\lambda)}(k_2)\varepsilon^{\nu(\lambda)}(k_2)\bar{u}^{(s_1)}(k_1)\gamma_\mu\,(\not{k}_1 + \not{k}_2 + m_t) \\ & (\cos\theta_{\tilde{t}} P_R - \sin\theta_{\tilde{t}} P_L) u^{(s_2)}(p_A)\bar{u}^{(s_2)}(p_A)(\cos\theta_{\tilde{t}} P_L - \sin\theta_{\tilde{t}} P_R)\,(\not{k}_1 + \not{k}_2 + m_t)\,\gamma_\nu u^{(s_1)}(k_1) \\ = & \frac{2\mathrm{g_s}^4}{(s - m_t^2)^2} \underbrace{\sum_{i,k,a,b} T^a_{kj} T^b_{ji} T^b_{ih} T^a_{hk}}_{\overline{|M_{s,\text{color}}|^2}} \sum_{s1,s2,\lambda} \varepsilon^{*\mu(\lambda)}(k_2)\varepsilon^{\nu(\lambda)}(k_2)\bar{u}^{(s_1)}(k_1)\gamma_\mu\,(\not{k}_1 + \not{k}_2 + m_t)\,(\cos\theta_{\tilde{t}} P_R - \sin\theta_{\tilde{t}} P_L) \\ & u^{(s_2)}(p_A)\bar{u}^{(s_2)}(p_A)(\cos\theta_{\tilde{t}} P_L - \sin\theta_{\tilde{t}} P_R)\,(\not{k}_1 + \not{k}_2 + m_t)\,\gamma_\nu u^{(s_1)}(k_1).\end{aligned} \tag{5.22}$$

We assume that physical gluons are massless so that $k_2 \cdot k_2 = 0$. The sum over polarizations λ only refers to the polarization vectors and can be performed using eq. (B.15).

$$\begin{aligned}\overline{|M_s|^2} = & \frac{2\mathrm{g_s}^4}{(s - m_t^2)^2} \overline{|M_{s,\text{color}}|^2} \sum_{s1,s2} (-g^{\mu\nu})\bar{u}^{(s_1)}(k_1)\gamma_\mu\,(\not{k}_1 + \not{k}_2 + m_t)\,(\cos\theta_{\tilde{t}} P_R - \sin\theta_{\tilde{t}} P_L) \\ & u^{(s_2)}(p_A)\bar{u}^{(s_2)}(p_A)(\cos\theta_{\tilde{t}} P_L - \sin\theta_{\tilde{t}} P_R)\,(\not{k}_1 + \not{k}_2 + m_t)\,\gamma_\nu u^{(s_1)}(k_1).\end{aligned} \tag{5.23}$$

It is appropriate to label the indices of matrix products explicitly to point out how we can continue the calculation. The summation over indices $\alpha, \beta, \delta \ldots$ is implied:

$$\begin{aligned}\overline{|M_s|^2} = & \frac{2\mathrm{g_s}^4}{(s - m_t^2)^2} \overline{|M_{s,\text{color}}|^2} (-g^{\mu\nu}) \sum_{s1,s2} [\bar{u}^{(s_1)}(k_1)]_\alpha [\gamma_\mu]_{\alpha\beta} [\not{k}_1 + \not{k}_2 + m_t]_{\beta\delta} [\cos\theta_{\tilde{t}} P_R - \sin\theta_{\tilde{t}} P_L]_{\delta\epsilon} \\ & [u^{(s_2)}(p_A)_\epsilon \bar{u}^{(s_2)}(p_A)_\phi][\cos\theta_{\tilde{t}} P_L - \sin\theta_{\tilde{t}} P_R]_{\phi\zeta} [\not{k}_1 + \not{k}_2 + m_t]_{\zeta\eta} [\gamma_\nu]_{\eta\theta} [u^{(s_1)}(k_1)]_\theta.\end{aligned} \tag{5.24}$$

The metric tensor is simply evaluated by raising either the index μ or ν of a remaining object and setting $\mu = \nu$. Because the matrix character is covered by the component, $[u^{(s_1)}(k_1)]_{(\theta)}$ can be shifted to the front. Now, one is able to perform the spin-summation by using the completeness relation for spinors u (see eq. (B.14)):

$$\begin{aligned}\overline{|M_s|^2} = &-\frac{2g_s^4}{(s-m_t^2)^2}\overline{|M_{s,\text{color}}|^2}\underbrace{\sum_{s1}[u^{(s_1)}(k_1)_\theta \bar{u}^{(s_1)_\alpha}(k_1)]}_{[\not{k}_1+m_t]_{\theta\alpha}}[\gamma^\mu]_{\alpha\beta}[\not{k}_1+\not{k}_2+m_t]_{\beta\delta}[\cos\theta_{\tilde{t}}P_R-\sin\theta_{\tilde{t}}P_L]_{\delta\epsilon}\\ &\underbrace{\sum_{s2}[u^{(s_2)}(p_A)_\epsilon \bar{u}^{(s_2)}(p_A)_\phi]}_{[\not{p}_A+m_{\tilde{g}}]_{\epsilon\phi}}[\cos\theta_{\tilde{t}}P_L-\sin\theta_{\tilde{t}}P_R]_{\phi\zeta}[\not{k}_1+\not{k}_2+m_t]_{\zeta\eta}[\gamma_\mu]_{\eta\theta}.\end{aligned} \tag{5.25}$$

Considering the indices of matrix multiplication, one notices that these multiplications end as a trace of the product of all matrices:

$$\begin{aligned}\overline{|M_s|^2} =&\frac{2g_s^4}{(s-m_t^2)^2}\overline{|M_{s,\text{color}}|^2}\text{Tr}\big[(\not{k}_1+m_t)\gamma^\mu(\not{k}_1+\not{k}_2+m_t)(\sin\theta_{\tilde{t}}P_L-\cos\theta_{\tilde{t}}P_R)\\ &(\not{p}_A+m_{\tilde{g}})(\cos\theta_{\tilde{t}}P_L-\sin\theta_{\tilde{t}}P_R)(\not{k}_1+\not{k}_2+m_t)\gamma_\mu\big].\end{aligned} \tag{5.26}$$

Using eq. (B.16) we can shift γ_μ to the front of the matrix products. Since m_t is scalar and commutes with everything, we obtain using eq. (B.6):

$$\begin{aligned}\overline{|M_s|^2} =&\frac{2g_s^4}{(s-m_t^2)^2}\overline{|M_{s,\text{color}}|^2}\text{Tr}\big[(\gamma_\mu\not{k}_1\gamma^\mu+4m_t)(\not{k}_1+\not{k}_2+m_t)(\sin\theta_{\tilde{t}}P_L-\cos\theta_{\tilde{t}}P_R)\\ &(\not{p}_A+m_{\tilde{g}})(\cos\theta_{\tilde{t}}P_L-\sin\theta_{\tilde{t}}P_R)(\not{k}_1+\not{k}_2+m_t)\big].\end{aligned} \tag{5.27}$$

The anticommutator for γ-matrices (see eq. (B.5)) and Feynman's slash notation gives eq. (5.28).

$$\begin{aligned}\gamma_\mu\not{k}_1\gamma^\mu &= \gamma_\mu k_1^\nu\gamma_\nu\gamma^\mu = k_1^\nu\gamma_\mu\gamma_\nu\gamma^\mu = k_1^\nu(2g_{\mu\nu}-\gamma_\nu\gamma_\mu)\gamma^\mu\\ &= 2k_{1,\mu}\gamma^\mu - 4k_1^\nu\gamma_\nu = -2\not{k}_1\end{aligned} \tag{5.28}$$

Accordingly, we can write:

$$\begin{aligned}\overline{|M_s|^2} =&\frac{2g_s^4}{(s-m_t^2)^2}\overline{|M_{s,\text{color}}|^2}\text{Tr}\big[(\not{k}_1+\not{k}_2+m_t)(-2\not{k}_1+4m_t)(\not{k}_1+\not{k}_2+m_t)(\sin\theta_{\tilde{t}}P_L-\cos\theta_{\tilde{t}}P_R)\\ &(\not{p}_A+m_{\tilde{g}})(\cos\theta_{\tilde{t}}P_L-\sin\theta_{\tilde{t}}P_R)\big].\end{aligned} \tag{5.29}$$

Expanding the first two brackets in the trace and making use of eq. (B.8), we can continue the calculation of the trace in order to use trace theorems in the end(see eq. (5.30)). Since most traces containing γ^5 vanish, we expand the other terms at first and multiply the brackets containing γ^5s in the end.

$$\begin{aligned}\overline{|M_s|^2} =&\frac{2g_s^4}{(s-m_t^2)^2}\overline{|M_{s,\text{color}}|^2}\text{Tr}\big[(-2k_1^2-2\not{k}_2\not{k}_1+2m_t\not{k}_1+4m_t(\not{k}_2+m_t))(\not{k}_1+\not{k}_2+m_t)(\sin\theta_{\tilde{t}}P_L-\cos\theta_{\tilde{t}}P_R)\\ &(\not{p}_A+m_{\tilde{g}})(\cos\theta_{\tilde{t}}P_L-\sin\theta_{\tilde{t}}P_R)\big]\end{aligned} \tag{5.30}$$

Expanding again, one obtains by using eq. (B.8):

$$\begin{aligned}\overline{|M_s|^2} =&\frac{2g_s^4}{(s-m_t^2)^2}\overline{|M_{s,\text{color}}|^2}\text{Tr}\big[(-2k_1^2\not{k}_1 - 2k_1^2\not{k}_2 + 2m_t k_1^2 + 4m_t(\not{k}_2\not{k}_1 + m_t\not{k}_1) - 2k_1^2\not{k}_2 - 2\not{k}_2\not{k}_1\not{k}_2\\ &+ 2m_t\not{k}_1\not{k}_2 + 4m_t(k_2^2 + m_t\not{k}_2) + m_t\cdot(-2k_1^2 - 2\not{k}_2\not{k}_1 + 2m_t\not{k}_1 + 4m_t\not{k}_2 + 4m_t^2))\\ &(\sin\theta_{\tilde{t}}P_L - \cos\theta_{\tilde{t}}P_R)(\not{p}_A + m_{\tilde{g}})(\cos\theta_{\tilde{t}}P_L - \sin\theta_{\tilde{t}}P_R)\big] \qquad (5.31)\\ =&\frac{2g_s^4}{(s-m_t^2)^2}\overline{|M_{s,\text{color}}|^2}\text{Tr}\big[(-2k_1^2\not{k}_1 - 4k_1^2\not{k}_2 + 2m_t\not{k}_2\not{k}_1 + 6m_t^2\not{k}_1 - 2\not{k}_2\not{k}_1\not{k}_2 + 2m_t\not{k}_1\not{k}_2 + 4m_t k_2^2\\ &+ 8m_t^2\not{k}_2 + 4m_t^3)(\sin\theta_{\tilde{t}}P_L - \cos\theta_{\tilde{t}}P_R)(\not{p}_A + m_{\tilde{g}})(\cos\theta_{\tilde{t}}P_L - \sin\theta_{\tilde{t}}P_R)\big]. \qquad (5.32)\end{aligned}$$

Giving a closer look to $\not{k}_2\not{k}_1\not{k}_2$, we again make use of the anti-commutation relation for γ-matrices:

$$\begin{aligned}\not{k}_2\not{k}_1\not{k}_2 =&\gamma^\mu\gamma^\nu\gamma^\lambda k_{2,\mu}k_{1,\nu}k_{2,\lambda}\\ =&(2g^{\mu\nu}\gamma^\lambda - \gamma^\nu\gamma^\mu\gamma^\lambda)k_{2,\mu}k_{1,\nu}k_{2,\lambda}\\ =&2(k_2\cdot k_1)\not{k}_2 - k_2^2\not{k}_1. \qquad (5.33)\end{aligned}$$

Since the squared momenta are the associated squared masses , $k_1^2 = m_t^2$ and $k_2^2 = 0$. Additionally, we take advantage of eq. (5.33):

$$\begin{aligned}\overline{|M_s|^2} =&\frac{2g_s^4}{(s-m_t^2)^2}\overline{|M_{s,\text{color}}|^2}\text{Tr}\big[(+4m_t^2\not{k}_1 + 4m_t^2\not{k}_2 + 2m_t\not{k}_2\not{k}_1 - \underline{2\not{k}_2\not{k}_1\not{k}_2} + 2m_t\not{k}_1\not{k}_2 + \cancel{4m_t k_2^2} + 4m_t^3)\\ &(\sin\theta_{\tilde{t}}P_L - \cos\theta_{\tilde{t}}P_R)(\not{p}_A + m_{\tilde{g}})(\cos\theta_{\tilde{t}}P_L - \sin\theta_{\tilde{t}}P_R)\big]\\ =&\frac{2g_s^4}{(s-m_t^2)^2}\overline{|M_{s,\text{color}}|^2}\text{Tr}\big[(+4m_t^2\not{k}_1 + 4m_t^2\not{k}_2 + 2m_t\not{k}_2\not{k}_1 + \underline{\cancel{2k_2^2}\not{k}_1 - 4(k_2\cdot k_1)\not{k}_2} + 2m_t\not{k}_1\not{k}_2 + 4m_t^3)\\ &(\sin\theta_{\tilde{t}}P_L - \cos\theta_{\tilde{t}}P_R)(\not{p}_A + m_{\tilde{g}})(\cos\theta_{\tilde{t}}P_L - \sin\theta_{\tilde{t}}P_R)\big]. \qquad (5.34)\end{aligned}$$

One has to consider the terms containing the chirality operators $P_L = \frac{1}{2}(1-\gamma^5)$ and $P_R = \frac{1}{2}(1+\gamma^5)$. Using $P_L\cdot P_R = P_R\cdot P_L = 0$ and $P_i^2 = P_i$ (see eq. (B.12)), we get eq. (5.35). One can shift $\not{p}_A$ to the front by using the anti-commutation of γ^μ and γ^5 which leads to e.g.: $P_L\not{p}_A = \not{p}_A P_R$.

$$\begin{aligned}&(\sin\theta_{\tilde{t}}P_L - \cos\theta_{\tilde{t}}P_R)(\not{p}_A + m_{\tilde{g}})(\cos\theta_{\tilde{t}}P_L - \sin\theta_{\tilde{t}}P_R)\\ =&\not{p}_A(\sin\theta_{\tilde{t}}P_R - \cos\theta_{\tilde{t}}P_L)(\cos\theta_{\tilde{t}}P_L - \sin\theta_{\tilde{t}}P_R)\\ &+ m_{\tilde{g}}(\sin\theta_{\tilde{t}}P_L - \cos\theta_{\tilde{t}}P_R)(\cos\theta_{\tilde{t}}P_L - \sin\theta_{\tilde{t}}P_R)\\ =&\not{p}_A(-\sin^2\theta_{\tilde{t}}P_R - \cos^2\theta_{\tilde{t}}P_L) + m_{\tilde{g}}(\sin\theta_{\tilde{t}}\cos\theta_{\tilde{t}}P_L + \sin\theta_{\tilde{t}}\cos\theta_{\tilde{t}}P_R)\\ =&-\not{p}_A\cdot\frac{1}{2}\cdot[\sin^2\theta_{\tilde{t}}(1+\gamma^5) + \cos^2\theta_{\tilde{t}}(1-\gamma^5)] + m_{\tilde{g}}\sin\theta_{\tilde{t}}\cos\theta_{\tilde{t}}(P_L+P_R)\\ =&-\frac{1}{2}\cdot\not{p}_A(1+\sin^2\theta_{\tilde{t}}\gamma^5 - \cos^2\theta_{\tilde{t}}\gamma^5) + m_{\tilde{g}}\sin\theta_{\tilde{t}}\cos\theta_{\tilde{t}}\\ =&\frac{1}{2}\big(-\not{p}_A + \not{p}_A\cos(2\theta_{\tilde{t}})\gamma^5 + m_{\tilde{g}}\sin(2\theta_{\tilde{t}})\big) \qquad (5.35)\end{aligned}$$

We can utilize eq. (5.35) directly:

$$\begin{aligned}\overline{|M_s|^2} =&\frac{2g_s^4}{(s-m_t^2)^2}\overline{|M_{s,\text{color}}|^2}\text{Tr}\big[(+2m_t^2\not{k}_1 + 2m_t^2\not{k}_2 + m_t\not{k}_2\not{k}_1 - 2(k_2\cdot k_1)\not{k}_2 + m_t\not{k}_1\not{k}_2 + 2m_t^3)\\ &\big(-\not{p}_A + \not{p}_A\cos(2\theta_{\tilde{t}})\gamma^5 + m_{\tilde{g}}\sin(2\theta_{\tilde{t}})\big)\big]. \qquad (5.36)\end{aligned}$$

Now, we need to consider the trace theorems (see appendix B.1). Since traces of an odd number of Dirac matrices vanish, such terms will be neglected taken into account that slashed momenta are sums of γ^μ-matrices with a prefactor. Additionally, in context of not multiplying more than four γ^μ's and one γ^5 matrix, we can neglect all traces containing γ^5 except for traces of the product of four slashed momenta and one γ^5(see eq. (B.23)). Since the trace is a linear transformation, we obtain eq. (5.37).

$$\begin{aligned}\overline{|M_s|^2} =& \frac{2g_s^4}{(s-m_t^2)^2}\overline{|M_{s,\text{color}}|^2}\Big(\text{Tr}\big[-2m_t^2 \not{k}_1 \not{p}_A\big] - \text{Tr}\big[2m_t^2 \not{k}_2 \not{p}_A\big] + \text{Tr}\big[m_{\tilde{g}} m_t \sin(2\theta_{\tilde{t}}) \not{k}_2 \not{k}_1\big] + \text{Tr}\big[2(k_2\cdot k_1)\not{k}_2 \not{p}_A\big] \\ &+ \text{Tr}\big[m_t m_{\tilde{g}} \sin(2\theta_{\tilde{t}}) \not{k}_1 \not{k}_2\big] + \text{Tr}\big[2m_t^3 m_{\tilde{g}} \sin(2\theta_{\tilde{t}})\big]\Big) \end{aligned} \tag{5.37}$$

The traces can be evaluated using $\text{Tr}(1) = 4$(eq. (B.17)) and $\text{Tr}\big(\not{a}\not{b}\big) = 4a\cdot b$(eq. (B.18)):

$$\begin{aligned}\overline{|M_s|^2} =& \frac{8g_s^4}{(s-m_t^2)^2}\overline{|M_{s,\text{color}}|^2}\big[-2m_t^2(k_1\cdot p_A) - 2m_t^2(k_2\cdot p_A) + m_{\tilde{g}} m_t \sin(2\theta_{\tilde{t}})(k_2\cdot k_1) + 2(k_2\cdot k_1)(k_2\cdot p_A) \\ &+ m_t m_{\tilde{g}} \sin(2\theta_{\tilde{t}})(k_1\cdot k_2) + 2m_t^3 m_{\tilde{g}} \sin(2\theta_{\tilde{t}})\big] \\ =& \frac{16g_s^4}{(s-m_t^2)^2}\overline{|M_{s,\text{color}}|^2}\big[-m_t^2(k_1\cdot p_A) - m_t^2(k_2\cdot p_A) + (k_2\cdot k_1)(k_2\cdot p_A) \\ &+ m_t m_{\tilde{g}} \sin(2\theta_{\tilde{t}})((k_1\cdot k_2) + m_t^2)\big]. \end{aligned} \tag{5.38}$$

Finally, one has to calculate the color part $\overline{|M_{s,\text{color}}|^2}$:

$$\overline{|M_{s,\text{color}}|^2} = \sum_{i,k,a,b} T^a_{kj} T^b_{ji} T^b_{ih} T^a_{hk}. \tag{5.39}$$

The four T-matrices are linked by summation over j, i and h which produces matrix multiplications. Due to the summation over k these products are equal to the trace of the four T-matrices. We can make use of eq. (B.35) to calculate this trace:

$$\begin{aligned}\overline{|M_{s,\text{color}}|^2} =& \sum_{a,b} \text{Tr}\Big(T^a T^b T^b T^a\Big) \\ =& \frac{1}{12}\delta^{ab}\delta^{ba} + \frac{1}{8} h^{abn} h^{nba}. \end{aligned} \tag{5.40}$$

Permuting the indices of h in respect to eq. (B.28), we get eq. (5.41) and calculate $h^{abn}h^{ban}$ by making use of eq. (B.31). The Kronecker deltas are evaluated too. Since a and b are the colors of gluon and gluino, $\delta^{aa} = 8$.

$$\overline{|M_{s,\text{color}}|^2} = \frac{1}{12}\delta^{aa} + \frac{1}{8} h^{abn} h^{ban} \tag{5.41}$$

$$= \frac{1}{12}\cdot 8 + \frac{1}{8}\cdot\frac{112}{3} = \frac{16}{3}. \tag{5.42}$$

To finish the calculation of $\overline{|M_s|^2}$, except for averaging factors, one can insert eq. (5.42) into eq. (5.38) and obtains:

$$\overline{|M_s|^2} = \frac{16^2 g_s^4}{3(s-m_t^2)^2}\big[-m_t^2(k_1\cdot p_A) - m_t^2(k_2\cdot p_A) + (k_2\cdot k_1)(k_2\cdot p_A) + m_t m_{\tilde{g}} \sin(2\theta_{\tilde{t}})((k_1\cdot k_2) + m_t^2)\big]. \tag{5.43}$$

5.2.3. Squared invariant amplitude of t-channel

Proceeding with the calculation of $\overline{|M|^2}$ we calculate $\overline{|M_t|^2}$ using eqs. (5.12) and (5.19) and sum over external degrees of freedom:

$$\begin{aligned}
\overline{|M_t|^2} =& \sum_{i,k,a,b,s_1,s_2,\lambda} \frac{\sqrt{2}g_s^2 T^b_{kl} T^a_{li} \varepsilon^{*\mu(\lambda)}(k_2)}{t-m^2_{\tilde{t}_1}} \bar{u}^{(s_1)}(k_1)\left((\cos\theta_{\tilde{t}} P_R - \sin\theta_{\tilde{t}} P_L)\right) u^{(s_2)}(p_A)(2p_B - k_2)_\mu \\
& \frac{\sqrt{2}g_s^2 T^b_{hk} T^a_{ih} \varepsilon^{\nu(\lambda)}(k_2)}{t-m^2_{\tilde{t}_1}} (2p_B - k_2)_\nu \bar{u}^{(s_2)}(p_A)(\cos\theta_{\tilde{t}} P_L - \sin\theta_{\tilde{t}} P_R) u^{(s_1)}(k_1) \\
=& \frac{2g_s^4}{(t-m^2_{\tilde{t}_1})^2} \sum_{i,k,a,b} T^b_{kl} T^a_{li} T^b_{hk} T^a_{ih} \sum_\lambda \varepsilon^{*\mu(\lambda)}(k_2)\varepsilon^{\nu(\lambda)}(k_2) \sum_{s_1,s_2} \bar{u}^{(s_1)}(k_1)\left((\cos\theta_{\tilde{t}} P_R - \sin\theta_{\tilde{t}} P_L)\right) \\
& u^{(s_2)}(p_A)(2p_B - k_2)_\mu (2p_B - k_2)_\nu \bar{u}^{(s_2)}(p_A)(\cos\theta_{\tilde{t}} P_L - \sin\theta_{\tilde{t}} P_R) u^{(s_1)}(k_1).
\end{aligned} \tag{5.44}$$

The summation over T^i matrices leads to the same trace like in the calculation of $\overline{|M_s|^2}$. Furthermore, we again use eq. (B.15) to perform the sum over the polarizations of the polarization vectors. Shifting $u^{(s_1)}(k_1)$ to the front and using that $(2p_B - k_2)_\eta$ is scalar, one can use the completeness relation (eq. (B.14)) and perform the summation over both spins s_1 and s_2. As before one obtains a trace of 4×4 matrices:

$$\begin{aligned}
\overline{|M_t|^2} =& \frac{2g_s^4}{(t-m^2_{\tilde{t}_1})^2} \underbrace{\sum_{a,b} \mathrm{Tr}\left(T^a T^b T^b T^a\right)}_{\frac{16}{3}} \underbrace{\sum_\lambda \varepsilon^{*\mu(\lambda)}(k_2)\varepsilon^{\nu(\lambda)}(k_2)}_{-g^{\mu\nu}} \mathrm{Tr}\Big[(\not{k}_1 + m_t)\left((\cos\theta_{\tilde{t}} P_R - \sin\theta_{\tilde{t}} P_L)\right) \\
& (2p_B - k_2)_\mu (2p_B - k_2)_\nu (\not{p}_A + m_{\tilde{g}})(\cos\theta_{\tilde{t}} P_L - \sin\theta_{\tilde{t}} P_R)\Big] \\
=& \frac{32g_s^4}{3(t-m^2_{\tilde{t}_1})^2} g^{\mu\nu}(2p_B - k_2)_\mu (2p_B - k_2)_\nu \mathrm{Tr}\Big[(\not{k}_1 + m_t)\left((\sin\theta_{\tilde{t}} P_L - \cos\theta_{\tilde{t}} P_R)\right) \\
& (\not{p}_A + m_{\tilde{g}})(\cos\theta_{\tilde{t}} P_L - \sin\theta_{\tilde{t}} P_R)\Big].
\end{aligned} \tag{5.45}$$

Evaluating the metric tensor and using eq. (5.35), we get:

$$\overline{|M_t|^2} = \frac{32g_s^4}{3(t-m^2_{\tilde{t}_1})^2}(2p_B - k_2)^2 \mathrm{Tr}\Big[(\not{k}_1 + m_t)\frac{1}{2}\left(-\not{p}_A + \not{p}_A \cos(2\theta_{\tilde{t}})\gamma^5 + m_{\tilde{g}} \sin(2\theta_{\tilde{t}})\right)\Big]. \tag{5.46}$$

Since traces of the products of one or two γ^μ's and one γ^5 vanish, the expression can be simplified by dropping the term involving γ^5. Additionally, the trace of the product of an odd number of γ^μ's vanishes:

$$\begin{aligned}
\overline{|M_t|^2} =& \frac{16g_s^4}{3(t-m^2_{\tilde{t}_1})^2}(2p_B - k_2)^2 \mathrm{Tr}\Big[(\not{k}_1 + m_t)\left(-\not{p}_A + m_{\tilde{g}} \sin(2\theta_{\tilde{t}})\right)\Big] \\
=& \frac{16g_s^4}{3(t-m^2_{\tilde{t}_1})^2}(2p_B - k_2)^2 \mathrm{Tr}\Big[-\not{k}_1 \not{p}_A + m_t m_{\tilde{g}} \sin(2\theta_{\tilde{t}})\Big].
\end{aligned} \tag{5.47}$$

The traces are evaluated using again eq. (B.18) and eq. (B.17). Regarding to gluons being massless, k_2^2 vanishes. Moreover, p_B is the momentum of incoming scalar top so $p_B^2 = m^2_{\tilde{t}_1}$. One obtains eq. (5.48) for $\overline{|M_t|^2}$.

$$\overline{|M_t|^2} = \frac{16g_s^4}{3(t-m^2_{\tilde{t}_1})^2}(2p_B - k_2)^2\left[-4(k_1 \cdot p_A) + 4m_t m_{\tilde{g}} \sin(2\theta_{\tilde{t}})\right]$$

$$
\begin{aligned}
&= \frac{16 g_s^4}{3(t - m_{\tilde{t}_1}^2)^2} (4p_B^2 - 4(p_B \cdot k_2) + \cancel{k_2^2}) \left[-4(k_1 \cdot p_A) + 4 m_t m_{\tilde{g}} \sin(2\theta_{\tilde{t}}) \right] \\
&= \frac{16^2 g_s^4}{3(t - m_{\tilde{t}_1}^2)^2} \left[-m_{\tilde{t}_1}^2 (k_1 \cdot p_A) + (p_B \cdot k_2)(k_1 \cdot p_A) + m_t m_{\tilde{g}} \sin(2\theta_{\tilde{t}}) \left(m_{\tilde{t}_1}^2 - (p_B \cdot k_2) \right) \right]
\end{aligned} \tag{5.48}
$$

5.2.4. Squared invariant amplitude of u-channel

Furthermore, we need to calculate the squared amplitude for the u-channel $\overline{|M_u|^2}$ by again summing over external degrees of freedom of M_u (see eq. (5.13)) times $M_u^\dagger$(see eq. (5.20)):

$$
\begin{aligned}
\overline{|M_u|^2} = &\sum_{i,k,a,b,s_1,s_2,\lambda} \frac{-i\sqrt{2} g_s^2 T_{ki}^c f^{acb} \varepsilon^{*\mu(\lambda)}(k_2)}{u - m_{\tilde{g}}^2} \bar{u}^{(s_1)}(k_1) \left((\cos\theta_{\tilde{t}} P_R - \sin\theta_{\tilde{t}} P_L) \right) (\not{k}_1 - \not{p}_B + m_{\tilde{g}}) \gamma_\mu \\
&u^{(s_2)}(p_A) \frac{+i\sqrt{2} g_s^2 T_{ik}^d f^{adb} \varepsilon^{\nu(\lambda)}(k_2)}{u - m_{\tilde{g}}^2} \bar{u}^{(s_2)}(p_A) \gamma_\nu (\not{k}_1 - \not{p}_B + m_{\tilde{g}}) (\cos\theta_{\tilde{t}} P_L - \sin\theta_{\tilde{t}} P_R) u^{(s_1)}(k_1) \\
= &\frac{2 g_s^4}{(u - m_{\tilde{g}}^2)^2} \sum_{i,k,a,b} T_{ki}^c T_{ik}^d f^{acb} f^{adb} \sum_{\lambda} \varepsilon^{*\mu(\lambda)}(k_2) \varepsilon^{\nu(\lambda)}(k_2) \sum_{s_1,s_2} \bar{u}^{(s_1)}(k_1) (\cos\theta_{\tilde{t}} P_R - \sin\theta_{\tilde{t}} P_L) \\
&(\not{k}_1 - \not{p}_B + m_{\tilde{g}}) \gamma_\mu u^{(s_2)}(p_A) \bar{u}^{(s_2)}(p_A) \gamma_\nu (\not{k}_1 - \not{p}_B + m_{\tilde{g}}) (\cos\theta_{\tilde{t}} P_L - \sin\theta_{\tilde{t}} P_R) u^{(s_1)}(k_1).
\end{aligned} \tag{5.49}
$$

The sum over polarizations and spins can be performed as before by eq. (B.15) and eq. (B.14). For the color sums, we notice that the product $T_{ik}^d T_{ki}^c$ gives a trace:

$$
\begin{aligned}
\overline{|M_u|^2} = &\frac{2 g_s^4}{(u - m_{\tilde{g}}^2)^2} \operatorname{Tr}\left(T^c T^d \right) f^{acb} f^{adb} \operatorname{Tr}\Big[(\not{k}_1 + m_t)(\sin\theta_{\tilde{t}} P_L - \cos\theta_{\tilde{t}} P_R)(\not{k}_1 - \not{p}_B + m_{\tilde{g}}) \gamma_\mu \\
&(\not{p}_A + m_{\tilde{g}}) \gamma^\mu (\not{k}_1 - \not{p}_B + m_{\tilde{g}}) (\cos\theta_{\tilde{t}} P_L - \sin\theta_{\tilde{t}} P_R) \Big].
\end{aligned} \tag{5.50}
$$

The trace of T-matrices is caluclated by eq. (B.33) and the Kronecker δ is evaluated. The product of the structure constants with intended summations is evaluated by eq. (B.36). Furthermore, we shift $cos\theta_{\tilde{t}} P_L - \sin\theta_{\tilde{t}} P_R$ to the front of the trace:

$$
\begin{aligned}
\overline{|M_u|^2} = &\frac{2 g_s^4}{(u - m_{\tilde{g}}^2)^2} \underbrace{\operatorname{Tr}\left(T^c T^d \right)}_{\frac{1}{2}\delta^{cd}} f^{acb} f^{adb} \operatorname{Tr}\Big[(\cos\theta_{\tilde{t}} P_L - \sin\theta_{\tilde{t}} P_R)(\not{k}_1 + m_t)(\sin\theta_{\tilde{t}} P_L - \cos\theta_{\tilde{t}} P_R) \\
&(\not{k}_1 - \not{p}_B + m_{\tilde{g}}) \gamma_\mu (\not{p}_A + m_{\tilde{g}}) \gamma^\mu (\not{k}_1 - \not{p}_B + m_{\tilde{g}}) \Big] \\
= &\frac{2 g_s^4}{(u - m_{\tilde{g}}^2)^2} \frac{1}{2} \underbrace{f^{acb} f^{acb}}_{=24} \operatorname{Tr}\Big[(\cos\theta_{\tilde{t}} P_L - \sin\theta_{\tilde{t}} P_R)(\not{k}_1 + m_t)(\sin\theta_{\tilde{t}} P_L - \cos\theta_{\tilde{t}} P_R) \\
&(\not{k}_1 - \not{p}_B + m_{\tilde{g}}) \gamma_\mu (\not{p}_A + m_{\tilde{g}}) \gamma^\mu (\not{k}_1 - \not{p}_B + m_{\tilde{g}}) \Big].
\end{aligned} \tag{5.51}
$$

Analogue to eq. (5.35), one can calculate by again making use of the properties of chirality operators:

$$
\begin{aligned}
&(\cos\theta_{\tilde{t}} P_L - \sin\theta_{\tilde{t}} P_R)(\not{k}_1 + m_t)(\sin\theta_{\tilde{t}} P_L - \cos\theta_{\tilde{t}} P_R) \\
&\quad = m_t \sin\theta_{\tilde{t}} \cos\theta_{\tilde{t}} (P_L + P_R) - \sin^2\theta_{\tilde{t}} P_R \not{k}_1 - \cos^2\theta_{\tilde{t}} P_L \not{k}_1 \\
&\quad = m_t \sin\theta_{\tilde{t}} \cos\theta_{\tilde{t}} - \frac{1}{2}\not{k}_1 + \frac{1}{2}\cos^2\theta_{\tilde{t}} \gamma^5 \not{k}_1 - \frac{1}{2}\sin^2\theta_{\tilde{t}} \gamma^5 \not{k}_1
\end{aligned} \tag{5.52}
$$

$$= \frac{1}{2}(m_t \sin(2\theta_{\tilde{t}}) - \not{k}_1 + \cos(2\theta_{\tilde{t}})\gamma^5 \not{k}_1). \tag{5.53}$$

Due to a, b and c being color indices of gluons and gluinos, they have 8 different color states and $\delta_{aa} = 8$. Additionally, we use eq. (5.53):

$$\overline{|M_u|^2} = \frac{12 g_s^4}{(u - m_{\tilde{g}}^2)^2} \mathrm{Tr}\Big[\left(m_t \sin(2\theta_{\tilde{t}}) - \not{k}_1 + \cos(2\theta_{\tilde{t}})\gamma^5 \not{k}_1\right) (\not{k}_1 - \not{p}_B + m_{\tilde{g}}) \gamma_\mu (\not{p}_A + m_{\tilde{g}}) \gamma^\mu (\not{k}_1 - \not{p}_B + m_{\tilde{g}}) \Big]. \tag{5.54}$$

One again uses eq. (5.28) to eliminate the γ^μ's:

$$\begin{aligned}\overline{|M_u|^2} = &\frac{12 g_s^4}{(u - m_{\tilde{g}}^2)^2} \mathrm{Tr}\Big[\left(m_t \sin(2\theta_{\tilde{t}}) - \not{k}_1 + \cos(2\theta_{\tilde{t}})\gamma^5 \not{k}_1\right) (\not{k}_1 - \not{p}_B + m_{\tilde{g}}) \\ &(-2\not{p}_A + 4m_{\tilde{g}})(\not{k}_1 - \not{p}_B + m_{\tilde{g}}) \Big]. \end{aligned} \tag{5.55}$$

Expanding the brackets except for the one containing γ^5 gives:

$$\begin{aligned}\overline{|M_u|^2} = &\frac{12 g_s^4}{(u - m_{\tilde{g}}^2)^2} \mathrm{Tr}\Big[\left(m_t \sin(2\theta_{\tilde{t}}) - \not{k}_1 + \cos(2\theta_{\tilde{t}})\gamma^5 \not{k}_1\right) (-2\not{k}_1 \not{p}_A + 2\not{p}_B \not{p}_A - 2m_{\tilde{g}} \not{p}_A + 4m_{\tilde{g}} \not{k}_1 \\ &- 4m_{\tilde{g}} \not{p}_B + 4m_{\tilde{g}}^2)(\not{k}_1 - \not{p}_B + m_{\tilde{g}}) \Big] \\ = &\frac{12 g_s^4}{(u - m_{\tilde{g}}^2)^2} \mathrm{Tr}\Big[\left(m_t \sin(2\theta_{\tilde{t}}) - \not{k}_1 + \cos(2\theta_{\tilde{t}})\gamma^5 \not{k}_1\right) \Big(\underline{-2\not{k}_1 \not{p}_A \not{k}_1} + 2\not{p}_B \not{p}_A \not{k}_1 - 2m_{\tilde{g}} \not{p}_A \not{k}_1 + 4m_{\tilde{g}} k_1^2 \\ &- 4m_{\tilde{g}} \not{p}_B \not{k}_1 + 4m_{\tilde{g}}^2 \not{k}_1 + 2\not{k}_1 \not{p}_A \not{p}_B - \underline{2\not{p}_B \not{p}_A \not{p}_B} + 2m_{\tilde{g}} \not{p}_A \not{p}_B - 4m_{\tilde{g}} \not{k}_1 \not{p}_B + 4m_{\tilde{g}} p_B^2 - 4m_{\tilde{g}}^2 \not{p}_B \\ &- 2m_{\tilde{g}} \not{k}_1 \not{p}_A + 2m_{\tilde{g}} \not{p}_B \not{p}_A - 2m_{\tilde{g}}^2 \not{p}_A + 4m_{\tilde{g}}^2 \not{k}_1 - 4m_{\tilde{g}}^2 \not{p}_B + 4m_{\tilde{g}}^3 \Big) \Big]. \end{aligned} \tag{5.56}$$

We can use eq. (5.33) in order to rearrange the underlined terms containing three γ-matrices where two slashed momenta are equal but are separated by another slashed momentum. Furthermore, some terms can be combined:

$$\begin{aligned}\overline{|M_u|^2} = &\frac{12 g_s^4}{(u - m_{\tilde{g}}^2)^2} \mathrm{Tr}\Big[\left(m_t \sin(2\theta_{\tilde{t}}) - \not{k}_1 + \cos(2\theta_{\tilde{t}})\gamma^5 \not{k}_1\right) \Big(\underline{-4(k_1 \cdot p_A)\not{k}_1 + 2k_1^2 \not{p}_A} + 2\not{p}_B \not{p}_A \not{k}_1 - 2m_{\tilde{g}} \not{p}_A \not{k}_1 \\ &+ 4m_{\tilde{g}} k_1^2 - 4m_{\tilde{g}} \not{p}_B \not{k}_1 + 8m_{\tilde{g}}^2 \not{k}_1 + 2\not{k}_1 \not{p}_A \not{p}_B \underline{-4(p_B \cdot p_A)\not{p}_B + 2p_B^2 \not{p}_A} + 2m_{\tilde{g}} \not{p}_A \not{p}_B - 4m_{\tilde{g}} \not{k}_1 \not{p}_B + 4m_{\tilde{g}} p_B^2 \\ &- 8m_{\tilde{g}}^2 \not{p}_B - 2m_{\tilde{g}} \not{k}_1 \not{p}_A + 2m_{\tilde{g}} \not{p}_B \not{p}_A - 2m_{\tilde{g}}^2 \not{p}_A + 4m_{\tilde{g}}^3 \Big) \Big]. \end{aligned} \tag{5.57}$$

The trace theorems are used when expanding the remaining brackets. Thus, vanishing traces are neglected:

$$\begin{aligned}\overline{|M_u|^2} = &\frac{12 g_s^4}{(u - m_{\tilde{g}}^2)^2} \mathrm{Tr}\Big[+4(k_1 \cdot p_A)k_1^2 - 2k_1^2 \not{k}_1 \not{p}_A - 2\not{k}_1 \not{p}_B \not{p}_A \not{k}_1 + 2\cos(2\theta_{\tilde{t}})\gamma^5 \not{k}_1 \not{p}_B \not{p}_A \not{k}_1 \\ &- 2m_{\tilde{g}} m_t \sin(2\theta_{\tilde{t}}) \not{p}_A \not{k}_1 + 4m_{\tilde{g}} k_1^2 m_t \sin(2\theta_{\tilde{t}}) - 4m_{\tilde{g}} m_t \sin(2\theta_{\tilde{t}}) \not{p}_B \not{k}_1 - 8m_{\tilde{g}}^2 k_1^2 - 2k_1^2 \not{p}_A \not{p}_B \\ &+ 2\cos(2\theta_{\tilde{t}})\gamma^5 \not{k}_1 \not{k}_1 \not{p}_A \not{p}_B + 4(p_B \cdot p_A)\not{k}_1 \not{p}_B - 2p_B^2 \not{k}_1 \not{p}_A + 2m_{\tilde{g}} m_t \sin(2\theta_{\tilde{t}}) \not{p}_A \not{p}_B - 4m_{\tilde{g}} m_t \sin(2\theta_{\tilde{t}}) \not{k}_1 \not{p}_B \\ &+ 4m_{\tilde{g}} m_t \sin(2\theta_{\tilde{t}}) p_B^2 + 8m_{\tilde{g}}^2 \not{k}_1 \not{p}_B - 2m_{\tilde{g}} m_t \sin(2\theta_{\tilde{t}}) \not{k}_1 \not{p}_A + 2m_{\tilde{g}} m_t \sin(2\theta_{\tilde{t}}) \not{p}_B \not{p}_A \\ &+ 2m_{\tilde{g}}^2 \not{k}_1 \not{p}_A + 4m_{\tilde{g}}^3 m_t \sin(2\theta_{\tilde{t}}) \Big] \end{aligned} \tag{5.58}$$

We again make use of the anti-commutation of γ^5 and slashed momenta and $\not{k}_1\not{k}_1 = k_1^2$. One establishes traces of one γ^5 and only two slashed momenta which vanish. Furthermore, the terms containing $m_{\tilde{g}} m_t \sin(2\theta_{\tilde{t}})$ are combined (see eq. (5.59)). The order of the matrices in the trace is again changed in of use eq. (B.16). Squared four-momenta can be replaced by the squared masses in order to achieve eq. (5.60).

$$\begin{aligned}\overline{|M_u|^2} =& \frac{12 g_s^4}{(u-m_{\tilde{g}}^2)^2} \operatorname{Tr}\Big[+4(k_1\cdot p_A)k_1^2 - 2k_1^2 \not{k}_1 \not{p}_A - 2\not{k}_1\not{p}_B\not{p}_A\not{k}_1 - 8m_{\tilde{g}}^2 k_1^2 - 2k_1^2\not{p}_A\not{p}_B + 4(p_B\cdot p_A)\not{k}_1\not{p}_B \\ & - 2p_B^2\not{k}_1\not{p}_A + 8m_{\tilde{g}}^2\not{k}_1\not{p}_B + 2m_{\tilde{g}}^2\not{k}_1\not{p}_A + m_{\tilde{g}} m_t \sin(2\theta_{\tilde{t}})\big(-2\not{p}_A\not{k}_1 + 4k_1^2 - 4\not{p}_B\not{k}_1 + 2\not{p}_A\not{p}_B \\ & - 4\not{k}_1\not{p}_B + 4p_B^2 - 2\not{k}_1\not{p}_A + 2\not{p}_B\not{p}_A + 4m_{\tilde{g}}^2\big)\Big] \qquad (5.59) \\ =& \frac{12 g_s^4}{(u-m_{\tilde{g}}^2)^2} \operatorname{Tr}\Big[+4m_t^2(k_1\cdot p_A) + 2(m_{\tilde{g}}^2 - m_{\tilde{t}_1}^2 - m_t^2)\not{k}_1\not{p}_A - 8m_{\tilde{g}}^2 m_t^2 - 4m_t^2\not{p}_A\not{p}_B \\ & + 4((p_B\cdot p_A) + 2m_{\tilde{g}}^2)\not{k}_1\not{p}_B + m_{\tilde{g}} m_t \sin(2\theta_{\tilde{t}})\big(-4\not{p}_A\not{k}_1 + 4m_t^2 - 8\not{p}_B\not{k}_1 + 4\not{p}_A\not{p}_B + 4m_{\tilde{t}_1}^2 + 4m_{\tilde{g}}^2\big)\Big] \qquad (5.60)\end{aligned}$$

Due to linearity of traces, one uses again eqs. (B.17) and (B.18) for evaluating the traces and obtains:

$$\begin{aligned}\overline{|M_u|^2} =& \frac{96 g_s^4}{(u-m_{\tilde{g}}^2)^2}\Big[(m_{\tilde{g}}^2 - m_{\tilde{t}_1}^2 + m_t^2)(k_1\cdot p_A) - 4m_{\tilde{g}}^2 m_t^2 - 2m_t^2(p_A\cdot p_B) + 2(p_B\cdot p_A)(k_1\cdot p_B) \\ & + 4m_{\tilde{g}}^2(k_1\cdot p_B) + 2m_{\tilde{g}} m_t \sin(2\theta_{\tilde{t}})\big(-(p_A\cdot k_1) + m_t^2 - 2(p_B\cdot k_1) + (p_A\cdot p_B) + m_{\tilde{t}_1}^2 + m_{\tilde{g}}^2\big)\Big]. \qquad (5.61)\end{aligned}$$

5.2.5. Interference of s- and t-channel

To finish the calculation of $\overline{|M|^2}$, it is necessary to calculate three interference terms. Firstly, we calculate $\overline{M_s M_t^\dagger}$ by multiplying eq. (5.11) with eq. (5.19) and summing over external spins, colors and polarization:

$$\begin{aligned}\overline{M_s M_t^\dagger} =& \sum_{i,k,a,b,s_1,s_2,\lambda} \frac{\sqrt{2} g_s^2 T^a_{kj} T^b_{ji} \varepsilon^{*\mu(\lambda)}(k_2)}{s-m_t^2} \bar{u}^{(s_1)}(k_1)\gamma_\mu\,(\not{k}_1 + \not{k}_2 + m_t)\,(\cos\theta_{\tilde{t}} P_R - \sin\theta_{\tilde{t}} P_L) u^{(s_2)}(p_A) \\ & \frac{\sqrt{2} g_s^2 T^b_{hk} T^a_{ih} \varepsilon^{\nu(\lambda)}(k_2)}{t-m_{\tilde{t}_1}^2}(2p_B - k_2)_\nu \bar{u}^{(s_2)}(p_A)(\cos\theta_{\tilde{t}} P_L - \sin\theta_{\tilde{t}} P_R) u^{(s_1)}(k_1) \\ =& \frac{2 g_s^4}{(s-m_t^2)(t-m_{\tilde{t}_1}^2)} \sum_{i,k,a,b} T^a_{kj} T^b_{ji} T^b_{hk} T^a_{ih} \sum_\lambda \varepsilon^{*\mu(\lambda)}(k_2)\varepsilon^{\nu(\lambda)}(k_2) \sum_{s_1,s_2} \bar{u}^{(s_1)}(k_1)\gamma_\mu(2p_B - k_2)_\nu \\ & (\not{k}_1 + \not{k}_2 + m_t)\,(\cos\theta_{\tilde{t}} P_R - \sin\theta_{\tilde{t}} P_L) u^{(s_2)}(p_A)\bar{u}^{(s_2)}(p_A)(\cos\theta_{\tilde{t}} P_L - \sin\theta_{\tilde{t}} P_R) u^{(s_1)}(k_1) \\ =& \frac{2 g_s^4}{(s-m_t^2)(t-m_{\tilde{t}_1}^2)} \operatorname{Tr}\Big(T^a T^b T^a T^b\Big)(-g^{\mu\nu}) \operatorname{Tr}\Big[(\not{k}_1 + m_t)\gamma_\mu(2p_B - k_2)_\nu\,(\not{k}_1 + \not{k}_2 + m_t) \\ & (\cos\theta_{\tilde{t}} P_R - \sin\theta_{\tilde{t}} P_L)(\not{p}_A + m_{\tilde{g}})(\cos\theta_{\tilde{t}} P_L - \sin\theta_{\tilde{t}} P_R)\Big]. \qquad (5.62)\end{aligned}$$

The trace of four T-matrices is calculated by making use of eq. (B.35). Additionally, the metric tensor can be applied and we again use eq. (5.35) to simplify the brackets containing chirality operators:

$$\overline{M_s M_t^\dagger} = \frac{2 g_s^4}{(s-m_t^2)(t-m_{\tilde{t}_1}^2)} \underbrace{\operatorname{Tr}\Big(T^a T^b T^a T^b\Big)}_{\frac{1}{12}\delta^{ab}\delta^{ab} + \frac{1}{8} h^{abn} h^{nab}} (-1) \operatorname{Tr}\Big[(\not{k}_1 + m_t)\gamma_\mu(2p_B - k_2)^\mu\,(\not{k}_1 + \not{k}_2 + m_t)$$

$$\frac{1}{2}\left(+\not{p}_A - \not{p}_A \cos(2\theta_{\tilde{t}})\gamma^5 - m_{\tilde{g}} \sin(2\theta_{\tilde{t}})\right)\Bigg]$$
$$= \frac{g_s^4}{(s-m_t^2)(t-m_{\tilde{t}_1}^2)}\left(-\frac{1}{12}\delta^{ab}\delta^{ab} - \frac{1}{8}h^{abn}h^{nab}\right) \mathrm{Tr}\Big[(\not{k}_1 + m_t)(2\not{p}_B - \not{k}_2)\,(\not{k}_1 + \not{k}_2 + m_t)$$
$$\left(+\not{p}_A - \not{p}_A \cos(2\theta_{\tilde{t}})\gamma^5 - m_{\tilde{g}} \sin(2\theta_{\tilde{t}})\right)\Big] \tag{5.63}$$

Using eq. (B.28) we can write $h^{nab} = h^{abn}$ and make use of eq. (B.30) to calculate the product $h^{abn}h^{abn}$. Appending one Kronecker delta gives $\delta^{ab}\delta^{ab} = \delta^{aa} = 8$. Furthermore, one expands the brackets of the Dirac traces:

$$\overline{M_s M_t^\dagger} = \frac{g_s^4}{(s-m_t^2)(t-m_{\tilde{t}_1}^2)}\left(-\frac{8}{12} + \frac{32}{3\cdot 8}\right) \mathrm{Tr}\Big[(2\not{k}_1\not{p}_B - \not{k}_1\not{k}_2 + 2m_t\not{p}_B - m_t\not{k}_2)\,(\not{k}_1 + \not{k}_2 + m_t)$$
$$\left(+\not{p}_A - \not{p}_A \cos(2\theta_{\tilde{t}})\gamma^5 - m_{\tilde{g}} \sin(2\theta_{\tilde{t}})\right)\Big]$$
$$= \frac{2g_s^4}{3(s-m_t^2)(t-m_{\tilde{t}_1}^2)} \mathrm{Tr}\Big[(2\not{k}_1\not{p}_B\not{k}_1 - \not{k}_1\not{k}_2\not{k}_1 + 2m_t\not{p}_B\not{k}_1 - m_t\not{k}_2\not{k}_1 + 2\not{k}_1\not{p}_B\not{k}_2 - k_2^2\not{k}_1 + 2m_t\not{p}_B\not{k}_2$$
$$- m_t k_2^2 + 2m_t\not{k}_1\not{p}_B - m_t\not{k}_1\not{k}_2 + 2m_t^2\not{p}_B - m_t^2\not{k}_2)\left(+\not{p}_A - \not{p}_A \cos(2\theta_{\tilde{t}})\gamma^5 - m_{\tilde{g}} \sin(2\theta_{\tilde{t}})\right)\Big]. \tag{5.64}$$

According to eq. (5.33), the terms containing three slashed momenta where two momenta are equal can be transformed:

$$\overline{M_s M_t^\dagger} = \frac{2g_s^4}{3(s-m_t^2)(t-m_{\tilde{t}_1}^2)} \mathrm{Tr}\Big[(4(k_1\cdot p_B)\not{k}_1 - 2k_1^2\not{p}_B - 2(k_1\cdot k_2)\not{k}_1 + k_1^2\not{k}_2 + 2m_t\not{p}_B\not{k}_1 - m_t\not{k}_2\not{k}_1$$
$$+ 2\not{k}_1\not{p}_B\not{k}_2 - \underbrace{k_2^2\not{k}_1}_{=0} + 2m_t\not{p}_B\not{k}_2 - \underbrace{m_t k_2^2}_{=0} + 2m_t\not{k}_1\not{p}_B - m_t\not{k}_1\not{k}_2 + 2m_t^2\not{p}_B - m_t^2\not{k}_2)$$
$$\left(+\not{p}_A - \not{p}_A \cos(2\theta_{\tilde{t}})\gamma^5 - m_{\tilde{g}} \sin(2\theta_{\tilde{t}})\right)\Big]. \tag{5.65}$$

Continue expanding with respect to the trace theorems, one obtains:

$$\overline{M_s M_t^\dagger} = \frac{2g_s^4}{3(s-m_t^2)(t-m_{\tilde{t}_1}^2)} \mathrm{Tr}\Big[4(k_1\cdot p_B)\not{k}_1\not{p}_A - 2k_1^2\not{p}_B\not{p}_A - 2(k_1\cdot k_2)\not{k}_1\not{p}_A + k_1^2\not{k}_2\not{p}_A - 2m_t m_{\tilde{g}} \sin(2\theta_{\tilde{t}})\not{p}_B\not{k}_1$$
$$+ m_t m_{\tilde{g}} \sin(2\theta_{\tilde{t}})\not{k}_2\not{k}_1 + 2\not{k}_1\not{p}_B\not{k}_2\not{p}_A - 2\cos(2\theta_{\tilde{t}})\not{k}_1\not{p}_B\not{k}_2\not{p}_A\gamma^5 - 2m_t m_{\tilde{g}} \sin(2\theta_{\tilde{t}})\not{p}_B\not{k}_2$$
$$- 2m_t m_{\tilde{g}} \sin(2\theta_{\tilde{t}})\not{k}_1\not{p}_B + m_t m_{\tilde{g}} \sin(2\theta_{\tilde{t}})\not{k}_1\not{k}_2 + 2m_t^2\not{p}_B\not{p}_A - m_t^2\not{k}_2\not{p}_A\Big]$$
$$= \frac{2g_s^4}{3(s-m_t^2)(t-m_{\tilde{t}_1}^2)} \mathrm{Tr}\Big[4(k_1\cdot p_B)\not{k}_1\not{p}_A - 2(k_1\cdot k_2)\not{k}_1\not{p}_A + 2\not{k}_1\not{p}_B\not{k}_2\not{p}_A - 2\cos(2\theta_{\tilde{t}})\not{k}_1\not{p}_B\not{k}_2\not{p}_A\gamma^5$$
$$+ 2m_t m_{\tilde{g}} \sin(2\theta_{\tilde{t}})\left(-2\not{p}_B\not{k}_1 + \not{k}_2\not{k}_1 - \not{p}_B\not{k}_2\right)\Big]. \tag{5.66}$$

The traces of two slashed momenta are evaluated as before. Calculating the term containing four slashed momenta is done by eq. (B.19). Moreover, for the trace of four slashed momenta and one γ^5, we use eq. (B.23):

$$\overline{M_s M_t^\dagger} = \frac{16g_s^4}{3(s-m_t^2)(t-m_{\tilde{t}_1}^2)}\Big[2(k_1\cdot p_B)(k_1\cdot p_A) - (k_1\cdot k_2)(k_1\cdot p_A) + (k_1\cdot p_B)(k_2\cdot p_A)$$
$$- (k_1\cdot k_2)(p_B\cdot p_A) + (k_1\cdot p_A)(p_B\cdot k_2) + i\cos(2\theta_{\tilde{t}})\varepsilon^{\mu\nu\lambda\sigma}k_{1,\mu}p_{B,\nu}k_{2,\lambda}p_{A,\sigma}$$

$$+ m_t m_{\tilde{g}} \sin(2\theta_{\tilde{t}})\big(-2(p_B \cdot k_1) + (k_2 \cdot k_1) - (p_B \cdot k_2)\big)\Bigg]. \tag{5.67}$$

Since we are interested in real parts of the interference terms, it is not necessary to evaluate the total antisymmetric ε-tensor. Lastly, one can calculate $2\mathrm{Re}(\overline{M_s M_t^\dagger})$ which is needed for the calculation of $\overline{|M|^2}$(see eq. (5.14)):

$$\begin{aligned}2\mathrm{Re}(\overline{M_s M_t^\dagger}) =& \frac{32 g_s^4}{3(s-m_t^2)(t-m_{\tilde{t}_1}^2)}\Big[2(k_1\cdot p_B)(k_1\cdot p_A) - (k_1\cdot k_2)(k_1\cdot p_A) + (k_1\cdot p_B)(k_2\cdot p_A)\\ &- (k_1\cdot k_2)(p_B\cdot p_A) + (k_1\cdot p_A)(p_B\cdot k_2) + m_t m_{\tilde{g}}\sin(2\theta_{\tilde{t}})\big(-2(p_B\cdot k_1) + (k_2\cdot k_1) - (p_B\cdot k_2)\big)\Big].\end{aligned} \tag{5.68}$$

5.2.6. Interference of t- and u-channel

To continue, one has to calculate $\overline{M_t M_u^\dagger}$:

$$\begin{aligned}\overline{M_t M_u^\dagger} =& \sum_{i,k,a,b,s_1,s_2,\lambda} \frac{\sqrt{2} g_s^2 T^b_{kl} T^a_{li} \varepsilon^{*\mu(\lambda)}(k_2)}{t-m_{\tilde{t}_1}^2} \bar{u}^{(s_1)}(k_1)(\cos\theta_{\tilde{t}} P_R - \sin\theta_{\tilde{t}} P_L) u^{(s_2)}(p_A)(2p_B - k_2)_\mu\\ &\frac{+i\sqrt{2} g_s^2 T^d_{ik} f^{adb} \varepsilon^{\nu(\lambda)}(k_2)}{u-m_{\tilde{g}}^2} \bar{u}^{(s_2)}(p_A)\gamma_\nu(\not{k}_1 - \not{p}_B + m_{\tilde{g}})(\cos\theta_{\tilde{t}} P_L - \sin\theta_{\tilde{t}} P_R) u^{(s_1)}(k_1)\\ =& \frac{i 2 g_s^4}{(t-m_{\tilde{t}_1}^2)(u-m_{\tilde{g}}^2)} \sum_{i,k,a,b} T^b_{kl} T^a_{li} T^d_{ik} \underbrace{f^{adb}}_{=-f^{abd}} \underbrace{\sum_\lambda \varepsilon^{*\mu(\lambda)}(k_2)\varepsilon^{\nu(\lambda)}(k_2)}_{-g^{\mu\nu}} (2p_B - k_2)_\mu\\ &\mathrm{Tr}\Big[(\not{k}_1 + m_t)(\cos\theta_{\tilde{t}} P_R - \sin\theta_{\tilde{t}} P_L)(\not{p}_A + m_{\tilde{g}})\gamma_\nu(\not{k}_1 - \not{p}_B + m_{\tilde{g}})(\cos\theta_{\tilde{t}} P_L - \sin\theta_{\tilde{t}} P_R)\Big].\end{aligned} \tag{5.69}$$

Making use of the commutator for T-matrices $[T^a, T^b] = i f^{abd} T^d$ (see eq. (B.25)), we can replace $i f^{abd} T^d_{ik}$ by $T^a_{ij}T^b_{jk} - T^b_{ij}T^a_{jk}$. Since these products are multiplied by $T^b_{kl}T^a_{li}$, one sees that there are again matrix multiplications intended by the summation over l, i and j which end up in a trace by the summation over k. We obtain the difference of two traces of four 3×3 T-matrices:

$$\begin{aligned}\overline{M_t M_u^\dagger} =& \frac{2 g_s^4}{(t-m_{\tilde{t}_1}^2)(u-m_{\tilde{g}}^2)} \mathrm{Tr}\Big(T^b T^a T^a T^b - T^b T^a T^b T^a\Big)\\ &\mathrm{Tr}\Big[(\not{k}_1 + m_t)(\cos\theta_{\tilde{t}} P_R - \sin\theta_{\tilde{t}} P_L)(\not{p}_A + m_{\tilde{g}})(2\not{p}_B - \not{k}_2)(\not{k}_1 - \not{p}_B + m_{\tilde{g}})(\cos\theta_{\tilde{t}} P_L - \sin\theta_{\tilde{t}} P_R)\Big].\end{aligned} \tag{5.70}$$

Using eqs. (B.37) and (B.38), the products of four T-matrices with intended summation over a and b can be evaluated immediately. Since the difference of these two products equals $2\cdot \mathbb{1}_{3\times 3}$, the calculation of the trace results in the factor 3:

$$\begin{aligned}\overline{M_t M_u^\dagger} =& \frac{2 g_s^4}{(t-m_{\tilde{t}_1}^2)(u-m_{\tilde{g}}^2)} \mathrm{Tr}\Big(\frac{16}{9}\mathbb{1} + \frac{2}{9}\mathbb{1}\Big)\\ &\mathrm{Tr}\Big[(\cos\theta_{\tilde{t}} P_L - \sin\theta_{\tilde{t}} P_R)(\not{k}_1 + m_t)(\cos\theta_{\tilde{t}} P_R - \sin\theta_{\tilde{t}} P_L)(\not{p}_A + m_{\tilde{g}})(2\not{p}_B - \not{k}_2)(\not{k}_1 - \not{p}_B + m_{\tilde{g}})\Big].\end{aligned} \tag{5.71}$$

The terms containg chirality operators are simplified by making use of eq. (5.53). Furthermore, the other brackets of the Dirac trace are expanded:

$$\begin{aligned}\overline{M_t M_u^\dagger} =& \frac{2g_s^4}{(t-m_{\tilde{t}_1}^2)(u-m_{\tilde{g}}^2)} \cdot 6 \cdot \mathrm{Tr}\Bigg[\frac{1}{2}(\not{k}_1 - \cos(2\theta_{\tilde{t}})\gamma^5 \not{k}_1 - m_t \sin(2\theta_{\tilde{t}}))(\not{p}_A + m_{\tilde{g}})(2\not{p}_B - \not{k}_2) \\ & (\not{k}_1 - \not{p}_B + m_{\tilde{g}})\Bigg] \qquad (5.72)\\ =& \frac{6g_s^4}{(t-m_{\tilde{t}_1}^2)(u-m_{\tilde{g}}^2)} \mathrm{Tr}\Bigg[(\not{k}_1 - \cos(2\theta_{\tilde{t}})\gamma^5 \not{k}_1 - m_t \sin(2\theta_{\tilde{t}}))(2\not{p}_A\not{p}_B - \not{p}_A\not{k}_2 + 2m_{\tilde{g}}\not{p}_B - m_{\tilde{g}}\not{k}_2) \\ & (\not{k}_1 - \not{p}_B + m_{\tilde{g}})\Bigg] \\ =& \frac{6g_s^4}{(t-m_{\tilde{t}_1}^2)(u-m_{\tilde{g}}^2)} \mathrm{Tr}\Bigg[(\not{k}_1 - \cos(2\theta_{\tilde{t}})\gamma^5 \not{k}_1 - m_t \sin(2\theta_{\tilde{t}}))(2\not{p}_A\not{p}_B\not{k}_1 - \not{p}_A\not{k}_2\not{k}_1 + 2m_{\tilde{g}}\not{p}_B\not{k}_1 \\ & - m_{\tilde{g}}\not{k}_2\not{k}_1 - 2p_B^2\not{p}_A + \not{p}_A\not{k}_2\not{p}_B - 2m_{\tilde{g}}p_B^2 + m_{\tilde{g}}\not{k}_2\not{p}_B + 2m_{\tilde{g}}\not{p}_A\not{p}_B - m_{\tilde{g}}\not{p}_A\not{k}_2 + 2m_{\tilde{g}}^2\not{p}_B - m_{\tilde{g}}^2\not{k}_2)\Bigg]. \qquad (5.73)\end{aligned}$$

Making use of the trace theorems and anti-commutation of γ^5 and γ^μ, one obtains:

$$\begin{aligned}\overline{M_t M_u^\dagger} =& \frac{6g_s^4}{(t-m_{\tilde{t}_1}^2)(u-m_{\tilde{g}}^2)} \mathrm{Tr}\Bigg[2k_1^2\not{p}_A\not{p}_B - k_1^2\not{p}_A\not{k}_2 - 2p_B^2\not{k}_1\not{p}_A + \not{k}_1\not{p}_A\not{k}_2\not{p}_B - \cos(2\theta_{\tilde{t}})\gamma^5\not{k}_1\not{p}_A\not{k}_2\not{p}_B \\ & + 2m_{\tilde{g}}^2\not{k}_1\not{p}_B - m_{\tilde{g}}^2\not{k}_1\not{k}_2 + m_{\tilde{g}}m_t \sin(2\theta_{\tilde{t}})\big(-2\not{p}_B\not{k}_1 + \not{k}_2\not{k}_1 + 2p_B^2 - \not{k}_2\not{p}_B - 2\not{p}_A\not{p}_B + \not{p}_A\not{k}_2\big)\Bigg] \\ =& \frac{24g_s^4}{(t-m_{\tilde{t}_1}^2)(u-m_{\tilde{g}}^2)}\Bigg[2m_t^2(p_A\cdot p_B) - m_t^2(p_A\cdot k_2) - 2m_{\tilde{t}_1}^2(k_1\cdot p_A) + (k_1\cdot p_A)(k_2\cdot p_B) \\ & - (k_1\cdot k_2)(p_A\cdot p_B) + (k_1\cdot p_B)(p_A\cdot k_2) + i\cos(2\theta_{\tilde{t}})\varepsilon^{\mu\nu\lambda\sigma}k_{1,\mu}p_{A,\nu}k_{2,\lambda}p_{B,\sigma} + 2m_{\tilde{g}}^2(k_1\cdot p_B) \\ & - m_{\tilde{g}}^2(k_1\cdot k_2) + m_{\tilde{g}}m_t\sin(2\theta_{\tilde{t}})\big(-2p_B\cdot k_1 + k_2\cdot k_1 + 2m_{\tilde{t}_1}^2 - k_2\cdot p_B - 2p_A\cdot p_B + p_A\cdot k_2\big)\Bigg]. \qquad (5.74)\end{aligned}$$

Again, we have to calculate two times the real part of the interference term which leads to cancellation of the term containing the ε-tensor:

$$\begin{aligned}2\mathrm{Re}(\overline{M_t M_u^\dagger}) =& \frac{48g_s^4}{(t-m_{\tilde{t}_1}^2)(u-m_{\tilde{g}}^2)}\Bigg[2m_t^2(p_A\cdot p_B) - m_t^2(p_A\cdot k_2) - 2m_{\tilde{t}_1}^2(k_1\cdot p_A) + (k_1\cdot p_A)(k_2\cdot p_B) \\ & - (k_1\cdot k_2)(p_A\cdot p_B) + (k_1\cdot p_B)(p_A\cdot k_2) + 2m_{\tilde{g}}^2(k_1\cdot p_B) - m_{\tilde{g}}^2(k_1\cdot k_2) \\ & + m_{\tilde{g}}m_t\sin(2\theta_{\tilde{t}})\big(-2p_B\cdot k_1 + k_2\cdot k_1 + 2m_{\tilde{t}_1}^2 - k_2\cdot p_B - 2p_A\cdot p_B + p_A\cdot k_2\big)\Bigg]. \qquad (5.75)\end{aligned}$$

5.2.7. Interference of u- and s-channel

Finally, establishing the last interference term is necessary in order to evaluate $\overline{|M|^2}$.The summation over colors is done similarly to eqs. (5.70) and (5.71):

$$\begin{aligned}\overline{M_u M_s^\dagger} =& \sum_{i,k,a,b,s_1,s_2,\lambda} \frac{-i\sqrt{2}g_s^2 T_{ki}^c f^{acb}\varepsilon^{*\mu(\lambda)}(k_2)}{u-m_{\tilde{g}}^2}\bar{u}^{(s_1)}(k_1)(\cos\theta_{\tilde{t}}P_R - \sin\theta_{\tilde{t}}P_L)(\not{k}_1 - \not{p}_B + m_{\tilde{g}})\gamma_\mu u^{(s_2)}(p_A) \\ & \frac{\sqrt{2}g_s^2 T_{hk}^a T_{ih}^b \varepsilon^{\nu(\lambda)}(k_2)}{s-m_t^2}\bar{u}^{(s_2)}(p_A)(\cos\theta_{\tilde{t}}P_L - \sin\theta_{\tilde{t}}P_R)\,(\not{k}_1 + \not{k}_2 + m_t)\,\gamma_\nu u^{(s_1)}(k_1)\end{aligned}$$

$$
\begin{aligned}
=&\frac{2g_s^4}{(u-m_{\tilde{g}}^2)(s-m_t^2)} \underbrace{\sum_{i,k,a,b} T^b_{ih} T^a_{hk} i f^{acb} T^c_{ki}}_{=-6} (-g^{\mu\nu}) \operatorname{Tr}\Big[(\not{k}_1 + m_t)(\sin\theta_{\tilde{t}} P_L - \cos\theta_{\tilde{t}} P_R) \\
&(\not{k}_1 - \not{p}_B + m_{\tilde{g}})\gamma_\mu (\not{p}_A + m_{\tilde{g}})(\cos\theta_{\tilde{t}} P_L - \sin\theta_{\tilde{t}} P_R)(\not{k}_1 + \not{k}_2 + m_t)\gamma_\nu \Big] \\
=&\frac{12 g_s^4}{(u-m_{\tilde{g}}^2)(s-m_t^2)} \operatorname{Tr}\Big[(\not{k}_1 + m_t)(\sin\theta_{\tilde{t}} P_L - \cos\theta_{\tilde{t}} P_R)(\not{k}_1 - \not{p}_B + m_{\tilde{g}}) \\
&\gamma_\mu (\not{p}_A + m_{\tilde{g}})(\cos\theta_{\tilde{t}} P_L - \sin\theta_{\tilde{t}} P_R)(\not{k}_1 + \not{k}_2 + m_t)\gamma^\mu \Big]. \qquad (5.76)
\end{aligned}
$$

We take a closer look on the part $\gamma_\mu ....\gamma^\mu$ of the Dirac trace and would like to use $\gamma_\mu\gamma^\mu = 4$ and $\gamma_\mu \not{p} \gamma^\mu = -2\not{p}$(see eq. (5.28)) but the commutator $\{\gamma^\mu, \gamma^\nu\} = 2g^{\mu\nu}$ makes this rather long:

$$
\begin{aligned}
&\gamma_\mu (\not{p}_A + m_{\tilde{g}})(\cos\theta_{\tilde{t}} P_L - \sin\theta_{\tilde{t}} P_R)(\not{k}_1 + \not{k}_2 + m_t)\gamma^\mu \\
=&\gamma_\mu (\not{p}_A + m_{\tilde{g}})(\cos\theta_{\tilde{t}} P_L - \sin\theta_{\tilde{t}} P_R)(k_{1,\nu}\gamma^\nu\gamma^\mu + k_{2,\lambda}\gamma^\lambda\gamma^\mu + \gamma^\mu m_t) \\
=&\gamma_\mu (\not{p}_A + m_{\tilde{g}})(\cos\theta_{\tilde{t}} P_L - \sin\theta_{\tilde{t}} P_R)(2k_1^\mu - \gamma^\mu \not{k}_1 + 2k_2^\mu - \gamma^\mu \not{k}_2 + \gamma^\mu m_t) \\
=&\gamma_\mu (\not{p}_A + m_{\tilde{g}})\Big((2k_1^\mu - \gamma^\mu \not{k}_1 + 2k_2^\mu - \gamma^\mu \not{k}_2)(\cos\theta_{\tilde{t}} P_L - \sin\theta_{\tilde{t}} P_R) + \gamma^\mu m_t (\cos\theta_{\tilde{t}} P_R - \sin\theta_{\tilde{t}} P_L)\Big) \\
=&\big(\underbrace{2\not{k}_1\not{p}_A + 2\not{p}_A\not{k}_1}_{4p_A\cdot k_1} + 2\not{k}_2\not{p}_A + 2\not{p}_A\not{k}_2 + 2m_{\tilde{g}}\not{k}_1 - 4m_{\tilde{g}}\not{k}_1 + 2m_{\tilde{g}}\not{k}_2 - 4m_{\tilde{g}}\not{k}_2 \big)(\cos\theta_{\tilde{t}} P_L - \sin\theta_{\tilde{t}} P_R) \\
&+ \gamma_\mu (\not{p}_A + m_{\tilde{g}})\gamma^\mu m_t (\cos\theta_{\tilde{t}} P_R - \sin\theta_{\tilde{t}} P_L) \\
=&\big(4p_A\cdot k_1 + 4p_A\cdot k_2 - 2m_{\tilde{g}}\not{k}_1 - 2m_{\tilde{g}}\not{k}_2 \big)(\cos\theta_{\tilde{t}} P_L - \sin\theta_{\tilde{t}} P_R) \\
&+ (-2m_t \not{p}_A + 4m_{\tilde{g}} m_t)(\cos\theta_{\tilde{t}} P_R - \sin\theta_{\tilde{t}} P_L). \qquad (5.77)
\end{aligned}
$$

With help of eq. (5.77) one is able to continue the calculation of $\overline{M_u M_s^\dagger}$:

$$
\begin{aligned}
\overline{M_u M_s^\dagger} =&\frac{12 g_s^4}{(u-m_{\tilde{g}}^2)(s-m_t^2)} \operatorname{Tr}\Big[(\not{k}_1 + m_t)(\sin\theta_{\tilde{t}} P_L - \cos\theta_{\tilde{t}} P_R)(\not{k}_1 - \not{p}_B + m_{\tilde{g}}) \Big[\big(4p_A\cdot k_1 + 4p_A\cdot k_2 \\
&- 2m_{\tilde{g}}\not{k}_1 - 2m_{\tilde{g}}\not{k}_2 \big)(\cos\theta_{\tilde{t}} P_L - \sin\theta_{\tilde{t}} P_R) + (-2m_t\not{p}_A + 4m_{\tilde{g}} m_t)(\cos\theta_{\tilde{t}} P_R - \sin\theta_{\tilde{t}} P_L) \Big] \Big] \\
=&\frac{12 g_s^4}{(u-m_{\tilde{g}}^2)(s-m_t^2)} \operatorname{Tr}\Big[\Big[\big(4p_A\cdot k_1 + 4p_A\cdot k_2 - 2m_{\tilde{g}}\not{k}_1 - 2m_{\tilde{g}}\not{k}_2 \big)(\cos\theta_{\tilde{t}} P_L - \sin\theta_{\tilde{t}} P_R) \\
&+ (-2m_t\not{p}_A + 4m_{\tilde{g}} m_t)(\cos\theta_{\tilde{t}} P_R - \sin\theta_{\tilde{t}} P_L) \Big] (\not{k}_1 + m_t)(\sin\theta_{\tilde{t}} P_L - \cos\theta_{\tilde{t}} P_R)(\not{k}_1 - \not{p}_B + m_{\tilde{g}}) \Big]. \qquad (5.78)
\end{aligned}
$$

Moreover, we have to simplify the terms containing chirality operators. Therefore, it is convenient to calculate:

$$
\begin{aligned}
&(\cos\theta_{\tilde{t}} P_R - \sin\theta_{\tilde{t}} P_L)(\not{k}_1 + m_t)(\sin\theta_{\tilde{t}} P_L - \cos\theta_{\tilde{t}} P_R) \\
=&\not{k}_1 \cos\theta_{\tilde{t}} \sin\theta_{\tilde{t}} - m_t \Big(\frac{1}{2}(\cos^2\theta_{\tilde{t}} + \sin^2\theta_{\tilde{t}}) + \frac{1}{2}\gamma^5 (\cos^2\theta_{\tilde{t}} - \sin^2\theta_{\tilde{t}}) \Big) \\
=&\frac{1}{2}\Big(\not{k}_1 \sin(2\theta_{\tilde{t}}) - m_t - m_t\gamma^5 \cos(2\theta_{\tilde{t}}) \Big) \qquad (5.79)
\end{aligned}
$$

Continuing the calculation of $\overline{M_u M_s^\dagger}$ by expanding the terns using eqs. (5.53) and (5.79) gives:

$$\begin{aligned}
\overline{M_u M_s^\dagger} =& \frac{6g_s^4}{(u-m_{\tilde{g}}^2)(s-m_t^2)} \mathrm{Tr}\Big[\Big[\left(4p_A\cdot k_1 + 4p_A\cdot k_2 - 2m_{\tilde{g}}\not{k}_1 - 2m_{\tilde{g}}\not{k}_2\right)\left(m_t \sin(2\theta_{\tilde{t}}) - \not{k}_1 + \cos(2\theta_{\tilde{t}})\gamma^5\not{k}_1\right) \\
&+ \left(-2m_t\not{p}_A + 4m_{\tilde{g}}m_t\right)\Big(\not{k}_1 \sin(2\theta_{\tilde{t}}) - m_t - m_t\gamma^5\cos(2\theta_{\tilde{t}})\Big)\Big]\left(\not{k}_1 - \not{p}_B + m_{\tilde{g}}\right)\Big] \\
=& \frac{6g_s^4}{(u-m_{\tilde{g}}^2)(s-m_t^2)} \mathrm{Tr}\Big\{\Big[4(p_A\cdot k_1 + p_A\cdot k_2)\not{k}_1 - 2m_{\tilde{g}}k_1^2 - 2m_{\tilde{g}}\not{k}_1\not{k}_2 - 4(p_A\cdot k_1 + p_A\cdot k_2)\not{p}_B \\
&+ 2m_{\tilde{g}}\not{p}_B\not{k}_1 + 2m_{\tilde{g}}\not{p}_B\not{k}_2 + 4m_{\tilde{g}}(p_A\cdot k_1 + p_A\cdot k_2) - 2m_{\tilde{g}}^2\not{k}_1 - 2m_{\tilde{g}}^2\not{k}_2\Big]\left(m_t\sin(2\theta_{\tilde{t}})\right. \\
&\left. - \not{k}_1 + \cos(2\theta_{\tilde{t}})\gamma^5\not{k}_1\right) + \Big[-2m_t\not{k}_1\not{p}_A + 4m_{\tilde{g}}m_t\not{k}_1 + 2m_t\not{p}_B\not{p}_A - 4m_{\tilde{g}}m_t\not{p}_B - 2m_t m_{\tilde{g}}\not{p}_A \\
&+ 4m_{\tilde{g}}^2 m_t\Big]\left(\not{k}_1\sin(2\theta_{\tilde{t}}) - m_t - m_t\gamma^5\cos(2\theta_{\tilde{t}})\right)\Big\} \\
=& \frac{6g_s^4}{(u-m_{\tilde{g}}^2)(s-m_t^2)} \mathrm{Tr}\Big\{-4m_t^2(p_A\cdot k_1 + p_A\cdot k_2) + 4(p_A\cdot k_1 + p_A\cdot k_2)\not{p}_B\not{k}_1 + 2m_{\tilde{g}}^2 m_t^2 + 2m_{\tilde{g}}^2\not{k}_2\not{k}_1 \\
&+ m_{\tilde{g}}m_t\sin(2\theta_{\tilde{t}})\Big(-2m_t^2 - 2\not{k}_1\not{k}_2 + 2\not{p}_B\not{k}_1 + 2\not{p}_B\not{k}_2 + 4(p_A\cdot k_1 + p_A\cdot k_2) + 4m_t^2 - 4\not{p}_B\not{k}_1 \\
&- 2\not{p}_A\not{k}_1\Big) + 2m_t^2\not{k}_1\not{p}_A - 2m_t^2\not{p}_B\not{p}_A - 4m_{\tilde{g}}^2 m_t^2\Big\}. \qquad (5.80)
\end{aligned}$$

The non-vanishing traces can be evaluated and some terms are combined:

$$\begin{aligned}
\overline{M_u M_s^\dagger} =& \frac{48g_s^4}{(u-m_{\tilde{g}}^2)(s-m_t^2)}\Big\{-2m_t^2(p_A\cdot k_1 + p_A\cdot k_2) + 2(p_A\cdot k_1 + p_A\cdot k_2)(p_B\cdot k_1) + m_{\tilde{g}}^2 m_t^2 + m_{\tilde{g}}^2(k_2\cdot k_1) \\
&+ m_{\tilde{g}}m_t\sin(2\theta_{\tilde{t}})\Big(-m_t^2 - k_1\cdot k_2 + p_B\cdot k_1 + p_B\cdot k_2 + 2(p_A\cdot k_1 + p_A\cdot k_2) + 2m_t^2 - 2p_B\cdot k_1 \\
&- p_A\cdot k_1\Big) + m_t^2 k_1\cdot p_A - m_t^2 p_B\cdot p_A - 2m_{\tilde{g}}^2 m_t^2\Big\} \\
=& \frac{48g_s^4}{(u-m_{\tilde{g}}^2)(s-m_t^2)}\Big\{-m_t^2 p_A\cdot k_1 - 2m_t^2 p_A\cdot k_2 + 2(p_A\cdot k_1)(p_B\cdot k_1) + 2(p_A\cdot k_2)(p_B\cdot k_1) \\
&- m_{\tilde{g}}^2 m_t^2 + m_{\tilde{g}}^2(k_2\cdot k_1) - m_t^2 p_B\cdot p_A \\
&+ m_{\tilde{g}}m_t\sin(2\theta_{\tilde{t}})\Big(+m_t^2 - k_1\cdot k_2 - p_B\cdot k_1 + p_B\cdot k_2 + p_A\cdot k_1 + 2p_A\cdot k_2\Big)\Big\}. \qquad (5.81)
\end{aligned}$$

For the evaluation of $\overline{|M|^2}$ it is necessary to calculate $2\mathrm{Re}(\overline{M_u M_s^\dagger})$ which is in this case a multiplication with factor 2:

$$\begin{aligned}
2\mathrm{Re}(\overline{M_u M_s^\dagger}) =& \frac{96g_s^4}{(u-m_{\tilde{g}}^2)(s-m_t^2)}\Big\{-m_t^2 p_A\cdot k_1 - 2m_t^2 p_A\cdot k_2 + 2(p_A\cdot k_1)(p_B\cdot k_1) + 2(p_A\cdot k_2)(p_B\cdot k_1) \\
&- m_{\tilde{g}}^2 m_t^2 + m_{\tilde{g}}^2(k_2\cdot k_1) - m_t^2 p_B\cdot p_A \\
&+ m_{\tilde{g}}m_t\sin(2\theta_{\tilde{t}})\Big(+m_t^2 - k_1\cdot k_2 - p_B\cdot k_1 + p_B\cdot k_2 + p_A\cdot k_1 + 2p_A\cdot k_2\Big)\Big\}. \qquad (5.82)
\end{aligned}$$

5.3. Analytic result

Finally, the six calculated terms eqs. (5.43), (5.48), (5.61), (5.68), (5.75) and (5.82) need to be summed up and averaged over the degrees of freedom of incoming particles. Therefore, we divide by the factor $8\cdot 3\cdot 2 = 48$, where 8 results from eight possible color combinations for gluinos, 3 from the three possible color charges of squarks and 2 respects

the two different spin states of gluino as a spin-1/2 fermion:

$$\overline{|M|}^2 = \frac{1}{48}\left(\overline{|M_s|^2} + \overline{|M_t|^2} + \overline{|M_u|^2} + 2\mathrm{Re}(\overline{M_s M_t^\dagger}) + 2\mathrm{Re}(\overline{M_t M_u^\dagger}) + 2\mathrm{Re}(\overline{M_u M_s^\dagger})\right) \tag{5.83}$$

6. Numerical calculations

According to eq. (5.4), an integration over the element of solid angle $d\Omega$ is necessary in order to determine the total cross section. This is made by the numerical code **DM@NLO**[DMN].

The target of **DM@NLO** is to compute the annihilation cross section of the lightest neutralino in the MSSM more accurately and thus of the dark matter relic density. In the calculation of **DM@NLO** classes of processes like gaugino-squark co-annihilation into a quark and a gauge or Higgs boson are included. The code uses **SPheno 3.3.3** [Por03; PS12] as the spectrum generator for the calculation of the mass spectrum in MSSM. Furthermore, by working together with **micrOMEGAs 2.4**[Bel+11] the relic density is calculated.

The obtained result for the total cross section was compared with the result for co-annihilation of stop and neutralino under production of top and gluon [Har+15] which had been already implemented into **DM@NLO**. The couplings and propagators of s- and t-channel are identical for these processes. Because of that, one had to consider the different color factors and the mass of neutralino to compare the results for squared invariant amplitudes of s- and t-channel as well as their interference term. Additionally, results of **CalcHEP** for the total cross section were used to check the contribution of u-channel and the interference terms. By setting couplings to zero, it was possible to calculate the different contributions of the channels to the total cross section in **CalcHEP**.

Looking at the considered couplings of eqs. (A.1) to (A.5) again, we notice that the result of $|M|^2$ at tree-level can easily be generalized for a whole set of annihilations. The calculation can be transferred to co-annihilation of gluino with $\tilde{t}_2$ into top and gluon. This is done by considering the elements R_{2L} and R_{2R} of the mixing matrix in eq. (A.3) as well as the mass of $\tilde{t}_2$.

Furthermore, the calculation can be transmitted into co-annihilations of the scalar bottom quarks and gluino into a bottom quark and a gluon by replacing the masses of quark and squarks. This can also be done for the two other generations of quarks. Hence, the cross sections for a whole set of reactions has been established.

The solution to the Boltzmann equation considering the annihilation and co-annihilation of sparticles in use of eq. (3.22) is calculated numerically by **micrOMEGAs** for a scenario of the MSSM with the properties displayed in table 3. In total, 23 parameters are given to the spectrum creator **SPheno** to provide the associated mass spectrum. Using this mass spectrum, **DM@NLO** performs the necessary integration of differential cross section over the element of solid angle $d\Omega$ for different values of p_{cm}. As a result, the total cross section can be obtained.

micrOMEGAs takes all necessary annihilation cross sections and calculates the relic density of the neutralino using the given mass spectrum. The parameters of the scenario are chosen in such particular way that the result

Table 3: Scenario within the MSSM for the numerical calculation of the cross section. The dimensionful quantities are given in GeV. Only relevant parameters for this analysis are shown.

M_1	M_2	M_3	$M_{\tilde{q}_L}$	$M_{\tilde{t}_R}$	$M_{\tilde{b}_R}$	A_t	A_b	μ	m_{A^0}	$\tan\beta$	Q_{SUSY}
1400	2093.5	1267.2	2535	1395	3303.8	2755.3	2320.9	-3952.6	3624.8	15.5	1784.64

$m_{\tilde{\chi}_1^0}$	$m_{\tilde{\chi}_2^0}$	$m_{\tilde{\chi}_1^\pm}$	$m_{\tilde{t}_1}$	$m_{\tilde{b}_1}$	$m_{\tilde{g}}$	m_{h^0}	m_{H^0}	$\Omega_c h^2$
1401.5	2153.6	2153.5	1432.1	2554.2	1497.5	125.7	3625.2	0.1200

Table 4: Dominant annihilation channels and their contribution to relic density of neutralino in the scenario given in table 3. h refers to neutral Higgs bosons. Further processes contributing below 2% are left out.

Contributing processes	relative contribution
$\tilde{g}\,\tilde{t}_1 \;\rightarrow\; g\,t$	28.4%
$\tilde{g}\,\tilde{t}_1 \;\rightarrow\; W^+\,b$	5.5%
$\tilde{g}\,\tilde{t}_1 \;\rightarrow\; t\,h$	2.9%
$\tilde{g}\,\tilde{t}_1 \;\rightarrow\; Z^0\,t$	2.8%
$\tilde{t}_1\,\tilde{t}_1^* \;\rightarrow\; g\,g$	17.0%
$\tilde{t}_1\,\tilde{t}_1 \;\rightarrow\; t\,t$	13.6%
$\tilde{t}_1\,\tilde{t}_1^* \;\rightarrow\; \gamma\,g$	2.5%
$\tilde{g}\,\tilde{g} \;\rightarrow\; g\,g$	9.9%
$\tilde{\chi}_1^0\,\tilde{t}_1 \;\rightarrow\; g\,t$	5.6%

of **micrOMEGAs** equals the experimentally detected relic density of $\Omega_c h^2 = 0.120 \pm 0.001$ [Col+18]. Within this, **micrOMEGAs** has calculated the weight of the different processes contributing to the relic density. The contributions of the different annihilations are displayed in table 4.

The co-annihilation process $\tilde{g}\,\tilde{t}_1 \;\rightarrow\; g\,t$ dominates by contributing 28.4% to the relic density and is very important in this scenario. Annihilations of $\tilde{t}_1$ and $\tilde{t}_1^*$ are relevant too. The most important mechanism containing the LSP is the co-annihilation of $\tilde{\chi}_1^0$ and $\tilde{t}_1$ contributing 5.6% so the relic density - or number density of $\tilde{\chi}_1^0$ after "freezing out" - is highly sensitive to the density of $\tilde{t}_1$ according to the scenario. A quite similar scenario was studied in depth by S. Schmiemann et al. [Sch+19].

For the analysed scenario, we show the cross section at tree-level for co-annihilation of stop and gluino into top quark and gluon in fig. 7. The total cross section result is of the order $10^{-9}\mathrm{GeV}^{-2}$ for center-of-mass momenta p_{cm} between $10\,\mathrm{Gev}$ and $1000\,\mathrm{GeV}$. σ_{tree} slightly decreases with increasing p_{cm} but remains mostly constant. The total cross section is dominated by the gluino exchange of u-channel which is of the order $10^{-8}\mathrm{GeV}^{-2}$. Moreover, the interference of u and s-channel as well as the interference of u and t-channel result in a negative contribution of order $10^{-9}\mathrm{GeV}^{-2}$ which leads to σ_{tree} being of the order $10^{-9}\mathrm{GeV}^{-2}$. The s-channel contributes approximately $1 \cdot 10^{-9}\mathrm{GeV}^{-2}$ with a slightly decrease by increasing p_{cm}. If there was no u-channel exchange possible, the contribution of s-channel would dominate the cross section . Stop exchange of t-channel leads to a with p_{cm} increasing portion but its value is mostly lower than $3 \cdot 10^{-10}\mathrm{GeV}^{-2}$ and thus gives only a minor correction. Besides this, the interference between s and t-channel has an almost neglectable impact on the total cross section at tree level.

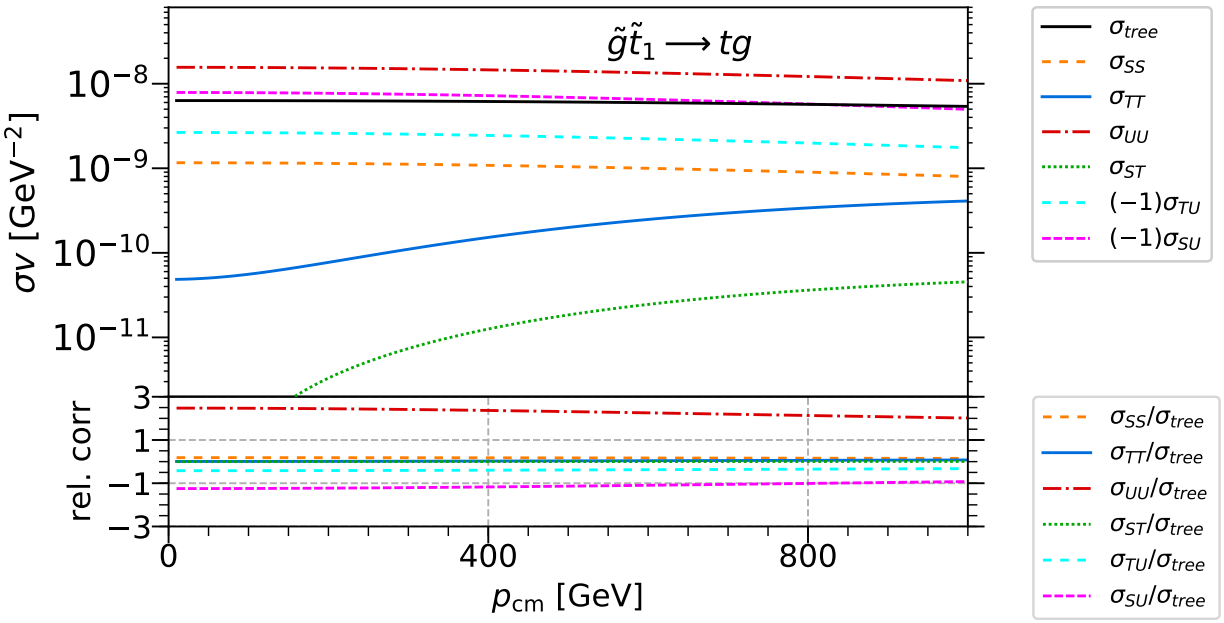

Figure 7: Calculated cross section for $\tilde{g}\,\tilde{t}_1 \longrightarrow g\,t$ at tree-level. Upper Part: Displayed are the total cross section times the Møller velocity of co-annihilating particles v and the contributions of channels and their interference terms to it as a function of center-of-mass momentum p_{cm}. σ_{tree} denotes the the total cross section at tree-level. The subscripts SS, TT, UU denote squared s, t and u channel respectively. ST, TU and SU refer to the contribution of the corresponding interference terms. Lower Part: Relative contributions to the total tree-level cross section.

7. Conclusion

After introducing into the field of dark matter and supersymmetric theories, the co-annihilation of a gluino and a stop into a top quark and gluon was studied since there are possible scenarios of the MSSM in which this process has a great impact. By establishing the relevant Feynman diagrams at tree-level for this process and applying the matching Feynman rules, the invariant amplitudes for these diagrams were set up. Furthermore, the calculation of the squared invariant amplitude under summation over external degrees of freedom was performed analytically. Finally, by implementing the resulting squared amplitude into a numerical code the total cross section was determined for a suitable scenario of the MSSM.

In conclusion, the co-annihilation of gluino and stop into top and gluon and its cross section at tree-level was determined successfully. In the analysed scenario of the MSSM the contribution of this process of 28.4% dominates the relic density thus small changes in this cross section have a great impact. Interestingly, the gluino exchange in the u-channel and corresponding interference terms have the largest impact on the cross section. Since this calculation was only done at tree-level, it might be important to study the next-to-leading order of perturbation theory for a more precise result. With more precise results for the masses and cross sections of sparticles, it might be more promising to search for hints in the data of experiments in the forecasted regions since masses and cross sections are observable. Even though the Minimal Supersymmetric Standard Model might not be the reality, the work on this thesis gave a comprehensive introduction into quantum field theory and physics beyond the Standard Model of particle physics. As a result, the work on this process and the Minimal Supersymmetric Standard Model builds a solid basis for further research in particle physics.

References

[Bel+11] G. Belanger et al. "Indirect search for dark matter with micrOMEGAs2.4". In: *Comput. Phys. Commun.* 182 (2011), pp. 842–856. DOI: 10.1016/j.cpc.2010.11.033. arXiv: 1004.1092 [hep-ph].

[BRS95] V. I. Borodulin, R. N. Rogalyov, and S. R. Slabospitsky. *CORE 2.1 (COmpendium of RElations, Version 2.1).* 1995. arXiv: hep-ph/9507456 [hep-ph].

[Col+18] Planck Collaboration et al. *Planck 2018 results. VI. Cosmological parameters.* 2018. arXiv: 1807.06209 [astro-ph.CO].

[ddC76] G. de Vaucouleurs, A. de Vaucouleurs, and J. R. Corwin. "Second reference catalogue of bright galaxies". In: *Second reference catalogue of bright galaxies* 1976 (Jan. 1976).

[DMN] DM@NLO. URL: https://dmnlo.hepforge.org (visited on 08/05/2020).

[Dod03] Scott Dodelson. *Modern Cosmology.* Amsterdam: Academic Press, 2003. ISBN: 978-0-12-219141-1.

[Ein09] Jaan Einasto. *Dark Matter.* 2009. arXiv: 0901.0632 [astro-ph.CO].

[FT97] Philippe Fischer and J. Anthony Tyson. "The Mass Distribution of the Most Luminous X-Ray Cluster RXJ 1347.5-1145 From Gravitational Lensing". In: *Astronomical Journal* 114 (July 1997), pp. 14–24. DOI: 10.1086/118447. arXiv: astro-ph/9703189 [astro-ph].

[GG91] Paolo Gondolo and Graciela Gelmini. "Cosmic abundances of stable particles: Improved analysis". In: *Nucl. Phys. B* 360 (1991), pp. 145–179. DOI: 10.1016/0550-3213(91)90438-4.

[Har+15] J. Harz et al. "One-loop corrections to neutralino-stop coannihilation revisited". In: *Phys. Rev. D* 91.3 (2015), p. 034028. DOI: 10.1103/PhysRevD.91.034028. arXiv: 1409.2898 [hep-ph].

[HM84] F. Halzen and Alan D. Martin. *QUARKS AND LEPTONS: AN INTRODUCTORY COURSE IN MODERN PARTICLE PHYSICS.* Jan. 1984. ISBN: 978-0-471-88741-6.

[JKG96] Gerard Jungman, Marc Kamionkowski, and Kim Griest. "Supersymmetric dark matter". In: *Physics Reports* 267.5-6 (Mar. 1996), pp. 195–373. ISSN: 0370-1573. DOI: 10.1016/0370-1573(95)00058-5. URL: http://dx.doi.org/10.1016/0370-1573(95)00058-5.

[Kra99] S. Kraml. *Stop and Sbottom Phenomenology in the MSSM.* 1999. arXiv: hep-ph/9903257 [hep-ph].

[MAR98] STEPHEN P. MARTIN. "A SUPERSYMMETRY PRIMER". In: *Advanced Series on Directions in High Energy Physics* (July 1998), pp. 1–98. ISSN: 1793-1339. DOI: 10.1142/9789812839657_0001. URL: http://dx.doi.org/10.1142/9789812839657_0001.

[MKR10] Richard Massey, Thomas Kitching, and Johan Richard. *The dark matter of gravitational lensing.* 2010. arXiv: 1001.1739 [astro-ph.CO].

[NN10] Y. Nagashima and Y. Nambu. *Elementary Particle Physics: Quantum Field Theory and Particles V1.* John Wiley & Sons, Ltd, 2010. ISBN: 9783527630097. URL: https://onlinelibrary.wiley.com/doi/book/10.1002/9783527630097.

[OP73] J. P. Ostriker and P. J. E. Peebles. "A Numerical Study of the Stability of Flattened Galaxies: or, can Cold Galaxies Survive?" In: *Astrophysical Journal* 186 (Dec. 1973), pp. 467–480. DOI: 10.1086/152513.

[Por03] Werner Porod. "SPheno, a program for calculating supersymmetric spectra, SUSY particle decays and SUSY particle production at e+ e- colliders". In: *Comput. Phys. Commun.* 153 (2003), pp. 275–315. DOI: 10.1016/S0010-4655(03)00222-4. arXiv: hep-ph/0301101.

[PS12] W. Porod and F. Staub. "SPheno 3.1: Extensions including flavour, CP-phases and models beyond the MSSM". In: *Comput. Phys. Commun.* 183 (2012), pp. 2458–2469. DOI: 10.1016/j.cpc.2012.05.021. arXiv: 1104.1573 [hep-ph].

[RW75] M. S. Roberts and R. N. Whitehurst. "The rotation curve and geometry of M31 at large galactocentric distances." In: *Astrophysical Journal* 201 (Oct. 1975), pp. 327–346. DOI: 10.1086/153889.

[Sch+19] S. Schmiemann et al. "Squark-pair annihilation into quarks at next-to-leading order". In: *Phys. Rev. D* 99.9 (2019), p. 095015. DOI: 10.1103/PhysRevD.99.095015. arXiv: 1903.10998 [hep-ph].

Appendices

In this thesis we use natural units of particle physics with $\hbar = c = \varepsilon_0 = k_B = 1$. Electric charges of particles are given with $e = 1$.

A. Feynman rules

Multiplicative factors for establishing $-iM$ [HM84, p. 149].
External Lines (in/out)

- spin 0 boson (or antiboson): **1**
- spin 1/2 fermion with momentum p and mass m: $\boldsymbol{u(p,m)}$ (in), $\boldsymbol{\bar{u}(p,m)}$ (out)
- spin 1/2 antifermion with momentum p and mass m: $\boldsymbol{\bar{v}(p,m)}$ (in), $\boldsymbol{v(p,m)}$ (out)
- spin 1 bosons of mass 0: $\boldsymbol{\varepsilon^{\mu}}$(in), $\boldsymbol{\varepsilon^{*\mu}}$(out)

Internal Lines - Propagators with mass m and momentum p
for color charged propagators one must multiply a Kronecker-delta in order to conserve its color

- spin 0 boson: $\frac{i}{p^2-m^2+i\epsilon}$
- spin 1/2 fermion: $\frac{i(\not{p}+m)}{p^2-m^2+i\epsilon}$

Vertex Factors used coupling factors according to [Kra99, p. 18-28]

- quark-gluon coupling

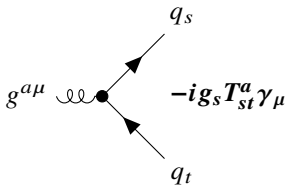

  - $\mathscr{L} = -g_s T^a_{st} G^a_\mu \bar{q}_s \gamma^\mu q_t$

(A.1)

- quark-squark-gluino couplings

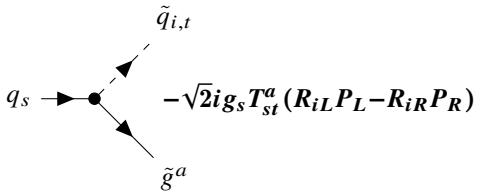

  - $\mathscr{L} = -\sqrt{2}g_sT^a_{st}[\bar{q}_s(R_{iL}P_R - R_{iR}P_L)$ $\tilde{g}^a\tilde{q}_{i,t} + \bar{\tilde{g}}^a(R_{iL}P_L - R_{iR}P_R)q_s\tilde{q}^*_{i,t}]$ (A.2)

  - rotation matrix R with mixing angle $\theta_{\tilde{q}}$ of squarks $\tilde{q}$

$$R = (R_{iL}, R_{iR}) \begin{pmatrix} \cos\theta_{\tilde{q}} & \sin\theta_{\tilde{q}} \\ -\sin\theta_{\tilde{q}} & \cos\theta_{\tilde{q}} \end{pmatrix}$$

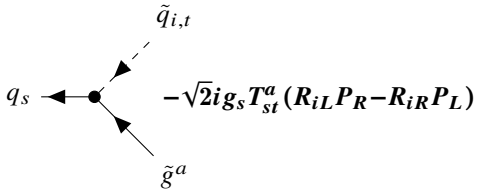

(A.3)

- gluon-squark coupling

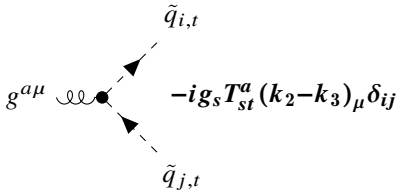

  - the momenta are determined by $g^a(k_1) \rightarrow \tilde{q}_i(k_2) + \bar{\tilde{q}}_j(k_3)$

  - $\mathscr{L} = -ig_sG^a_\mu T^a_{st}$ $\{\tilde{q}^*_{i,s}(\partial^\mu\tilde{q}_{i,t}) - (\partial^\mu\tilde{q}^*_{i,s})\tilde{q}_{i,t}\}$ (A.4)

- gluino-gluon coupling

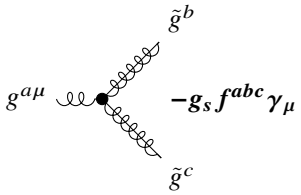

  - $\mathscr{L} = \frac{i}{2}g_sf^{abc}G^a_\mu\bar{\tilde{g}}^b\gamma^\mu\tilde{g}^c$

(A.5)

B. Formulae

Using the Pauli matrices $\boldsymbol{\sigma}$, the γ-matrices are in the Weyl representation given as:

$$\boldsymbol{\gamma} = \begin{pmatrix} 0 & \boldsymbol{\sigma} \\ -\boldsymbol{\sigma} & 0 \end{pmatrix}, \quad \gamma^0 = \begin{pmatrix} 0 & \mathbb{1} \\ \mathbb{1} & 0 \end{pmatrix}, \quad \gamma^5 = i\gamma^0\gamma^1\gamma^2\gamma^3 = \begin{pmatrix} -\mathbb{1} & 0 \\ 0 & \mathbb{1} \end{pmatrix}.$$

Useful formulas for evaluating squared amplitudes [HM84, p. 100-116]:

$$\bar{u}(p) = u^\dagger(p)\gamma^0, \tag{B.1}$$

$$\gamma^{\mu\dagger} = \gamma^0\gamma^\mu\gamma^0, \tag{B.2}$$

$$\gamma^0 \cdot \gamma^0 = \mathbb{1}_{4\times4}, \tag{B.3}$$

$$\gamma^{0\dagger} = \gamma^0, \tag{B.4}$$

$$\{\gamma^\mu, \gamma^\nu\} = 2g^{\mu\nu}\mathbb{1}_{4\times4}, \tag{B.5}$$
$$\gamma^\mu\gamma_\mu = 4 \tag{B.6}$$
$$\not{p} = \gamma_\mu p^\mu, \tag{B.7}$$
$$\not{p}\not{p} = p^2, \tag{B.8}$$
$$\gamma^{5\dagger} = \gamma^5, \qquad (\gamma^5)^2 = \mathbb{1}, \tag{B.9}$$
$$\{\gamma^5, \gamma^\mu\} = 0. \tag{B.10}$$

Properties of chirality operators P_R and P_L:

$$P_R = \frac{1}{2}(1+\gamma^5), \qquad P_L = \frac{1}{2}(1-\gamma^5), \tag{B.11}$$
$$P_L^2 = P_L, \qquad P_R^2 = P_R, \qquad P_L \cdot P_R = P_R \cdot P_L = 0, \tag{B.12}$$
$$P_L + P_R = \mathbb{1}. \tag{B.13}$$

Completeness relation for fermion spinors:

$$\sum_{s=1,2} u^{(s)}(p)\bar{u}^{(s)}(p) = \not{p} + m. \tag{B.14}$$

There are only two polarization states λ for massless vector bosons but it is allowed to sum over the unphysical polarization states too in case of this calculation. The completeness relation is given in the Feyman gauge:

$$\sum_\lambda \varepsilon^{*\mu(\lambda)}(k)\varepsilon^{\nu(\lambda)}(k) = -g^{\mu\nu}. \tag{B.15}$$

B.1. Trace theorems

Equations used for the evaluation of squared invariant amplitude[HM84, p. 123]:

$$\mathrm{Tr}(A \cdot B) = \mathrm{Tr}(B \cdot A) \tag{B.16}$$
$$\mathrm{Tr}(1) = 4 \tag{B.17}$$

Trace of odd number of γ^ν vanishes

$$\mathrm{Tr}\left(\not{a}\not{b}\right) = 4a \cdot b \tag{B.18}$$
$$\mathrm{Tr}\left(\not{a}\not{b}\not{c}\not{d}\right) = 4\{(a\cdot b)(c\cdot d) - (a\cdot c)(b\cdot d) + (a\cdot d)(b\cdot c)\} \tag{B.19}$$
$$\mathrm{Tr}\left(\gamma^5\right) = 0 \tag{B.20}$$
$$\mathrm{Tr}\left(\gamma^5\not{a}\not{b}\right) = 0 \tag{B.21}$$

$\epsilon^{\mu\nu\rho\sigma} = -\epsilon_{\mu\nu\rho\sigma}$ is the Levi-Civita anti-symmetric tensor[NN10, p. 819]:

$$\epsilon^{\mu\nu\rho\sigma} = \begin{cases} 1; & \mu\nu\rho\sigma = \text{even permutation of } 0123 \\ -1; & \mu\nu\rho\sigma = \text{odd permutation of } 0123 \\ 0; & \text{if two indices are the same} \end{cases} \tag{B.22}$$

One gets for the trace of four slashed momenta and one γ^5:

$$\mathrm{Tr}\left(\gamma^5 \not{a}\not{b}\not{c}\not{d}\right) = -i4\varepsilon^{\mu\nu\zeta\eta} a_\mu b_\nu c_\zeta d_\eta \tag{B.23}$$

B.2. Color-SU(3)

The 3×3 matrices $\lambda^a (a = 1, ...8)$ are generators of SU(3). We are working with $T^a = \frac{\lambda^a}{2}$. The prime characteristics of T^a are as follows(see chapter 8, [BRS95]):

$$T^{a\dagger} = T^a, \tag{B.24}$$

$$[T^a, T^b] = i f^{abc} T^c, \tag{B.25}$$

where f^{abc} are totally antisymmetric structure constants of SU(3). d^{abc} is a total symmetric tensor given by:

$$\{T^a, T^b\} = \frac{1}{3}\delta^{ab} + d^{abc} T^c. \tag{B.26}$$

An additional tensor h^{abc} can be introduced and has the following properties:

$$h^{abc} = d^{abc} + i f^{abc}, \tag{B.27}$$

$$h^{abc} = h^{bca} = h^{cab}, \tag{B.28}$$

$$h^{aab} = 0, \tag{B.29}$$

$$h^{abc} h^{abc} = -\frac{32}{3}, \tag{B.30}$$

$$h^{abc} h^{bac} = \frac{112}{3} \tag{B.31}$$

Some useful traces of T^a matrices:

$$\mathrm{Tr}(T^a) = 0 \tag{B.32}$$

$$\mathrm{Tr}\left(T^a T^b\right) = \frac{1}{2}\delta^{ab} \tag{B.33}$$

$$\mathrm{Tr}\left(T^a T^b T^c\right) = \frac{1}{4} h^{abc} \tag{B.34}$$

$$\mathrm{Tr}\left(T^a T^b T^c T^d\right) = \frac{1}{12}\delta^{ab}\delta^{cd} + \frac{1}{8} h^{abn} h^{ncd} \tag{B.35}$$

$$f^{akl} f^{bkl} = 3\delta^{ab} \tag{B.36}$$

$$T^a T^b T^a T^b = -\frac{2}{9}\mathbb{1} \tag{B.37}$$

$$T^a T^b T^b T^a = \frac{16}{9}\mathbb{1} \tag{B.38}$$